MASTER THESIS

COMPARING ADMITTANCE CONTROL LAWS FOR AN ACTIVE HEAD SUPPORT WITH HEALTHY SUBJECTS

Ingrid van den Heuvel

FACULTY OF ENGINEERING TECHNOLOGY
DEPARTMENT OF BIOMECHANICAL ENGINEERING

EXAMINATION COMMITTEE
Prof. Dr. Ir. H.F.J.M. Koopman
Ir. A.M. Geers, PDEng
Dr. Ir. M.N. Mahmood
Dr. E.C. Prinsen

DOCUMENT NUMBER
BW - 715

UNIVERSITY OF TWENTE.

19-02-2020

Summary

There are currently passive head supports on the market providing head and neck support for people with neuromuscular diseases. In this report, research into the control of an active head support has been performed. The performance of a control law, standard admittance, has been compared to the performance of the passive support. For this, a Fitts' like experiment with eight healthy subjects has been performed. Besides, a case study, with a second control law, variable admittance, has been carried out with two healthy subjects. In this case study, the performances of the standard admittance, variable admittance and passive head support were compared.

The control laws were designed in Simulink, MATLAB R2014b and communication with the device was via a real-time computer. Subjects were asked to move as fast and accurate as possible to virtual targets and they were asked to stay there. The possible targets were vertically arranged, corresponding to flexion and extension of the user's head and they appeared on a computer screen. As outcome parameters, movement time and overshoot were determined during the experiment. Additionally, muscle activity was measured with surface electromyography (Delsys Wireless Trigno). The activity of two muscles, sternocleidomastoid and the upper trapezius, was measured.

Results show that subjects had a higher movement time when performing the task with the standard admittance controller than with the passive device. However, results for muscle activity did not show significant differences. Overshoot was significantly higher for standard admittance than for the passive device. For standard admittance there was only a small indication that Fitts' law holds, because r-values were low compared to literature. The results for Fitts' law for the passive device were comparable with that of literature. For the case study, conflicting results were determined between the two subjects. Therefore no concluding statements can be made for variable admittance.

It is, however, questionable how reliable the results from this experiment are. Position of the head was measured by a potentiometer, which showed a lot of noise when the motor was enabled. Therefore, overshoot sometimes occurred due to the noise instead of actual head movements. This could have influenced the movement time and the linear fit as well. Besides, subjects could cause the motor to slip if they exerted a high torque on the device.

Extra offline research was performed to see if decreasing the dwell time would have an effect on the movement time and overshoot. Movement time and overshoot decreased for the standard admittance with a lower dwell time, however a significant difference in movement time was still present between standard admittance and the passive device.

In conclusion, with the current set-up, this admittance controller does not provide additional help compared to the passive device in moving the head in flexion-extension direction for subjects. It is advised to research the influence of the admittance controller when no slip is present and with better sensors. For variable admittance no conclusions can be drawn and research with more subjects would be insightful.

Samenvatting

Er zijn momenteel alleen passieve hoofdondersteuningen op de markt, die hood- en nekondersteuning bieden aan mensen met neuromusculaire aandoeningen. In dit verslag wordt een onderzoek gepresenteerd, waarin is gekeken naar de aansturing van een actieve hoofondersteuning. Het functioneren van een type aansturing, *standaard admittance*, is vergeleken met de passieve ondersteuning. Een experiment, vergelijkbaar met welke Fitts gebruikte in zijn onderzoek, is uitgevoerd met acht gezonde proefpersonen. Daarnaast is een case study uitgevoerd met een tweede type aansturing, *variabele admittance*, met twee proefpersonen. In deze case study zijn *standaard admittance*, *variabele admittance* en de passieve hoofdondersteuning met elkaar vergeleken.

Beide aansturingsmethoden waren ontworpen in Simulink, MATLAB R2014b and communicatie met de hoofdondersteuning ging via een real-time computer. Proefpersonen is gevraagd om zo snel en accuraat mogelijk naar een virtueel doelwit op een computerscherm te gaan en om daar te blijven. De mogelijke doelwitten waren op een verticale lijn georiënteerd, overeenkomend met flexie en extensie van het hoofd. Als onderzoeksvariabelen zijn bewegingstijd en *overshoot* bepaald tijdens het experiment. Daarnaast werd spieractiviteit gemeten met oppervlakte elektromyografie (Delsys Wireless Trigno). De activiteit van twee spieren, sternocleidomastoideus en de bovenste trapezius spier, was gemeten.

Resultaten laten zien dat proefpersonen een langere bewegingstijd hadden wanneer het experiment met de *standaard admittance* werd uitgevoerd dan wanneer het met de passive hoofdondersteuning werd gedaan. De spieractiviteit was, daarentegen, niet significant hoger voor *standaard admittance*. *Overshoot* was wel degelijk significant hoger voor *standaard admittance* dan voor de passive ondersteuning. Daarnaast is er een kleine indicatie dat Fitts' theorie houdt voor de *standaard admittance*, doordat de r-waarden lager waren dan die in de litatuur. Hoewel dit wel geldt voor de passieve ondersteuning, waar de r-waarden voor de passieve ondersteuning vergelijkbaar waren met die in de literatuur. Voor de case study zijn er tegenstrijdige resultaten, daarom kunnen er geen concluderende uitspraken worden gedaan.

Het is onduidelijk hoe betrouwbaar de resultaten van dit experiment zijn. De positie van het hoofd werd gemeten door de potentiometer die veel ruis had, wanneer de motor aanstond. Hierdoor kan het zijn dat de *overshoot* soms werd veroorzaakt door de ruis, in plaats van door echte bewegingen van het hoofd. Het is mogelijk dat deze ruis ook de bewegingstijd en de lineare fit heeft beïnvloed. Daarnaast konden proefpersonen slip van de motor creeëren door een hoge kracht op de ondersteuning uit te oefenen.

Extra offline onderzoek is gedaan om te zien of een kortere verblijfstijd invloed zou hebben op de bewegingstijd en de *overshoot*. Bewegingstijd en *overshoot* werd lager voor *standaard admittance* met een kortere verblijfstijd. Ondanks dit, was er nog steeds een significant verschil te zien tussen *standaard admittance* en de passieve ondersteuning.

Samengevat, binnen de huidige experiment opstelling helpt de *standaard admittance* aansturing de proefpersonen niet extra ten opzichte van de passieve ondersteuning bij het bewegen van het hoofd in flexie en extensie richting. Het wordt geadviseerd om de invloed van de *admittance* aansturing te testen wanneer er geen slip en minder ruis aanwezig is. Voor de *variabele admittance* kunnen er geen conclusies worden getrokken. Onderzoek met meer proefpersonen kan meer inzicht geven in het gebruik van deze aansturing.

Contents

Summary **3**

Samenvatting **4**

1 General introduction **7**
- 1.1 Admittance . . . 7
- 1.2 Fitts' law . . . 8
- 1.3 Thesis structure . . . 8

2 Research Paper **9**
- 2.1 Introduction . . . 10
- 2.2 Methods . . . 11
- 2.3 Results . . . 14
- 2.4 Discussion . . . 17
- 2.5 Conclusion and Future Recommendations . . . 19

3 General conclusion **22**

Appendices **23**

Appendix A Simulink model overview **24**
- A.1 Flowchart . . . 26
- A.2 Input Simulink & Processing . . . 27
  - A.2.1 Switch . . . 27
  - A.2.2 Potentiometer . . . 28
  - A.2.3 Encoder . . . 28
  - A.2.4 Force sensor . . . 29
  - A.2.5 EMG . . . 29
- A.3 Maximum Force . . . 30
- A.4 Force compensation . . . 30
- A.5 Normalizing Force . . . 31
- A.6 Control laws . . . 31
  - A.6.1 NC . . . 31
  - A.6.2 ADM . . . 31
  - A.6.3 VADM . . . 32
- A.7 Fitts' law . . . 33
- A.8 PID . . . 33
- A.9 Output Simulink . . . 33

Appendix B Calculations of the maximum speed of the motor and the head **35**

Appendix C Extra figures **36**
- C.1 Individual results muscle activity . . . 36
- C.2 Individual results subject 6 . . . 38
  - C.2.1 EMG . . . 38
  - C.2.2 Movement Time . . . 38
- C.3 Submaximal isometric contraction (SMIC) in flexion, extension direction . . . 39
- C.4 Individual figures overshoot case study . . . 41

C.5 Clarification overshoot 42
C.6 Movement time over time 43
C.7 Shorter dwell time 44
C.8 Slope comparison movement 49

Appendix D Information letter **50**

Appendix E Informed consent **53**

Appendix F Questionnaire subjects **56**

Appendix G Experimental protocol **57**

Bibliography **63**

Chapter 1

General introduction

People suffering from neuromuscular diseases (NMD) lose muscles force over time. They will often end up in a wheelchair, which makes daily activities more complex. Healthy people constantly move their head around, without much effort, but for people with NMD keeping their head up is already too much effort. Several head supports are on the market providing head and neck support for people with lesser muscle force, e.g. the Headmaster Collar (Symmetric designs) [1], the Savant Headrest (Neck solutions) [2] or Papillon (Focal Meditech) [3]. These devices are all passive, requiring the user to use their own muscle force if they want to move their head around. Because this can be too energy consuming for these patients, active head supports could be helpful. Research into active head supports has not yet been performed, but is required before bringing such supports on the market. In this thesis, the addition of a motor and force sensor to a passive head support, in combination with an admittance controller, is evaluated and researched. The question which will be answered by this thesis is: 'Can an active head support provide more support during movement if it is controlled with an admittance control law?' A standard admittance control law will be compared to the passive device in the main experiment. A second, variable admittance, control [5] will be compared with the standard admittance and passive device in a case study. The performance of these admittance controllers will be tested in a Fitts' like experiment. This experiment will be conducted with healthy subjects as a first step towards an active neck orthosis suitable for people with lesser muscle activity.

1.1 Admittance

If a user wants to control an active system, a control law is needed to manipulate the device. The control law takes the input of the user and converts it to the desired output, which is the (control) input of the system. In systems interacting with humans, these control laws are for example impedance or admittance control [4], which are each other's opposites. Impedance takes position as input and converts it to a force and admittance takes force as input and converts it to a motion. For several human segments such as; the trunk [5], the elbow [6, 7], the arm [8] or the lower extremity [9], admittance control has been successfully implemented. In the paper, in Chapter 2, it is therefore investigated whether admittance control can be implemented successfully on a head support as well.

As mentioned earlier, a control law takes an input and converts it to the desired output. For admittance this input is force and the output is either the desired, acceleration, velocity or position of the device. The standard equation for admittance, written in the Laplace domain is:

$$H = \frac{1}{ms^2 + bs + k} \tag{1.1}$$

Where m is the virtual inertia, b is the virtual damping and k is the virtual stiffness. With these variables, a virtual environment can be created in which systems feel lighter or heavier than in reality. Rewriting Equation 1.1 gives the following equation:

$$\ddot{\theta} = \frac{F_{in} - k\theta - b\dot{\theta}}{m} \tag{1.2}$$

Where F_{in} is the input force and θ, $\dot{\theta}$ and $\ddot{\theta}$ are respectively the desired position, velocity and acceleration. To get to position, two times the integral of Equation 1.2 is taken:

$$\theta = \int \int \ddot{\theta} \; d^2t \tag{1.3}$$

The above mentioned equations will be used in the implementation of the admittance control law in the paper. The parameters m, b and k will be determined using a pilot experiment. They will be kept constant for the standard admittance control law. Besides, a second control law, variable admittance control [5, 21] will be designed, with varying parameters. These parameters will change according to the event which takes place (acceleration or deceleration of the user's head).

1.2 Fitts' law

In the paper, presented in Chapter 2, a research is conducted with a Fitts' like experiment. This kind of experiment is associated with the experiment Fitts has performed in his paper *"The information capacity of the human motor system in controlling the amplitude of movement"* [10].

Fitts has researched the speed, amplitude, and accuracy trade-off in choice reaction time tasks, a task where every target requires another response [11]. He defined an index of difficulty for every task, based on their amplitude (A) and width (W):

$$ID(bits) = log_2(\frac{2A}{W}) \tag{1.4}$$

Based on the experiments he performed; which were a reciprocal tapping, a disc transfer and a pin transfer task, he proposed a law, which is currently known as Fitts' law [10]. This law shows a linear relation between the movement time and index of difficulty:

$$Movement\ Time = a + b \cdot log_2(\frac{2A}{W}) \tag{1.5}$$

where a and b are parameters depending on the task and subject.

In studies with human motion, it is often tested whether Fitts' law is applicable. For example, Fitts' law holds for arm movements [12–14] and trunk movements [5, 15]. Besides, Fitts' law holds in changed circumstances, such as underwater [14], extra damping [16] and with admittance and variable admittance control [5]. In Radwin et al. [17] and Jagacinsky et al. [12], they also found evidence that Fitts' law holds for head movements, which indicates that investigating Fitts' law in this experiment is useful as well.

The idea to make use of a Fitts like experiment came from Lenthe et al. [5]. In that paper, they compare admittance controllers and test whether Fitts' law holds for their controller.

1.3 Thesis structure

The main part of this report consist of a paper in which the earlier mentioned experiment will be explained and where results will be shown and discussed. After the paper, a general conclusion will be provided. In the appendices, the Simulink model is elaborated on, extra results of the experiment are displayed and the information letter, informed consent, questionnaire and experimental protocol are attached respectively.

Chapter 2

Research Paper

Comparing Admittance Control Laws for an Active Head Support with Healthy Subjects

Ingrid van den Heuvel

***Abstract*—To evaluate the addition of an admittance controller to a passive head support, a Fitts' like experiment has been performed on eight healthy subjects. Performance is evaluated by movement time, overshoot and muscle activity and it is investigated if Fitts' law holds. Subjects were asked to move as fast and accurate as possible towards a virtual target. Head flexion and extension corresponded to moving a cursor up and down a screen. A standard admittance control law with force as input was compared to the passive device. Besides, a case study was performed with two subjects with a second control law; variable admittance control. Results show that movement time has significantly increased when using standard admittance control. Besides, only a small indication that Fitts' law holds for standard admittance control is given by the linear fit. Furthermore, no difference in muscle activity has been noted between no control and standard admittance control. It is recommended to perform the main experiment once more with less noisy sensors, as this might lead to other conclusions. Regarding the variable admittance control law, no conclusions can be drawn as both subjects show varying results. Except for the movement time in extension direction, here it seems that movement time has increased for variable admittance control to standard admittance control. It is recommended to perform a study with a larger study sample to compare the variable admittance to the standard admittance.**

I. Introduction

Neuromuscular diseases (NMD) damage the functionality of the muscles. ALS (amyotrophic lateral scelerosis), SMA (spinal muscular atrophy) or MD (muscular dystrophy) are such diseases. In the Netherlands about 1500 people have ALS. [1] About 3 to 5 of 30.000 people have SMA in the Netherlands [2]. The most common form of MD: Duchenne (DMD), which occurs only in men, has an occurrence of about 1 in 3500 boys worldwide [3].

NMD progress over time and in general a lot of the patients end up in a wheelchair because of loss in muscle strength. Not only walking will become difficult, balancing your head can cost a lot of strength as well. A head is approximately 4.5 kg [4] and the muscles in the neck need to balance it against gravity. Therefore, daily activities such as eating, reading, looking around or using your phone can become difficult as well.

To overcome this issue, there are head supports and orthoses on the market providing support such as The Headmaster Collar (Symmetric designs) [5], the Savant Headrest (Neck solutions) [6] or Papillon (Focal Meditech) [7]. Unfortunately these devices do either not allow movement of the head, do restrict jaw movements, do not allow freedom of movement in all directions or do not provide support while moving their head, therefore limiting the patients freedom. For DMD patients, it is shown for muscles in the extremities that using these muscles might slow down the deterioration of these muscles [8]. This may also be valid for neck muscles. Besides, having the freedom to move your head around may increase the independence for wheelchair-bound people during the day. Therefore allowing patients to move their head is of importance.

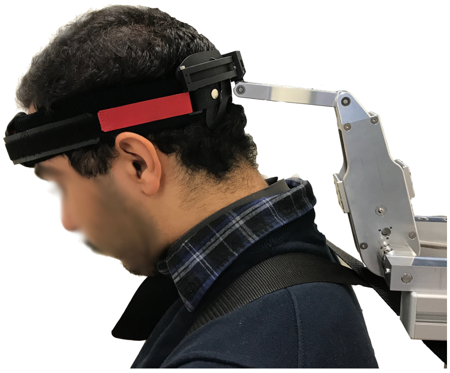

Fig. 1: Head orthosis attached to subject [9]

A new passive head support, allowing movement in flexion-extension and left and right rotation, is developed by Mahmood et al. [9] The head support has a head pad with a belt to attach the head to the device (see Figure 1). In this way the jaw is not restricted. The device is adjustable for every patient. The stiffness of the spring can be adjusted to support heavier or lighter heads and the system can be adjusted for neck height.

The passive head support has a novel balancing mechanism, balancing the head, in flexion-extension direction, against gravity. This device showed potential for a decrease in muscle activity for the upper trapezius and sternocleidomastoid when used by healthy subjects [9]. However, because it is fully passive, moving the device to other angles can cost too much energy for patients with weaker muscles.

To further improve the orthosis, a force sensor and motor have been added to the device for the flexion-extension direction. For an active system interacting with humans, a control law such as impedance or admittance is needed [10]. These control laws convert the input of the user to a desired output (control input of the system), respectively position to force and force to position. For several human segments such as; the trunk [11], the elbow [12], [13], the arm [14] and the lower extremity [15], admittance control has already been successfully implemented. In this study, it is investigated, whether admittance control can be successfully implemented for the head as well. In this study. the input for the admittance control will be the force exerted by the user's head and the output will be rotation of the motor in the flexion-extension direction.

In this paper the performance of a standard admittance controller is evaluated with a Fitts' like experiment (see Section II-E *Task*) and compared with the system in passive condition. The hypotheses are:

1) The standard admittance will lead to a decreased movement time compared to no control.
2) There is no significant difference for overshoot count for standard admittance and no control.
3) Fitts' law holds for the admittance control law.
4) With the standard admittance, the muscle activity is decreased during movement compared to no control.

Besides, a case study with a variable admittance control [11] is performed as well. For this case study it is expected that:

1) The variable admittance controller will have a decreased movement time compared to the standard admittance and no control.
2) With the variable admittance controller the muscle activity will be lower compared to standard admittance and no control.

In the next section, the method of the experiment and the case study will be explained. Also the design of the control laws will be discussed. Thereafter, the results are displayed for both the main experiment and the case study. In the subsequent section, the results are discussed and at last, the conclusion and future recommendations are described.

II. METHODS

The experiment was performed at the University of Twente. Ethical approval was given by the ethical committee EWI/ET (ref. no. RP 2019-71).

A. Participants

For this experiment, healthy participants were selected. Only subjects with no self-reported impairments concerning the neck and shoulder muscles participated. Additionally, the subjects had good vision (with or without additional glasses/lenses) in order to see the visual cues on the screen (0.5 m).

A total of eight subjects (five women, three men) participated in this experiment. The age of the participants was 22.25 $\pm$ 2.49 years and they had an average length of 177 $\pm$ 9 cm. All participants signed an informed consent (Appendix E). The main experiment, with two conditions, lasted approximately 1.5 hours. The case study, where two participants performed the experiment with three conditions, lasted 2 hours.

B. Experimental set-up

The subject was seated in a wheelchair at the beginning of the experiment. The head support, mounted on the back of the wheelchair, was connected to the subject's head with a belt and tightened to limit slip between the head and head support. The head support was adjusted in height and angle in such a way that the subject had a neutral head position (subject can look straight forward). Besides, the stiffness of the head support was adjusted in such a way that the subject's head was balanced against gravity (when the subject relaxed their neck muscles, their head would be kept in the same position by the device). The subject's movements were constricted with a belt over the chest to limit the movements of the upper body. In front of the wheelchair a display was placed on which the target and the subject controlled cursor were displayed. The subject had a safety button in their hand in case of emergency.

C. Hardware set-up

The motor (DCX22S GB KL 24V), planetary gearhead (GPX26HP 243:1) and encoder (ENX16 EASY 1024IMP) used in this set up are by Maxon motors. The potentiometer, which measures absolute angle position of the device, is from Metallux (Conductive plastic hollow shaft sensor PGL 60) and the force sensor, for the input force, is from Schunk (FT16459). All sensors were connected to an electronics box. Besides, a switch button (to change states during the experiment) and an emergency button were connected to the box as well. Inside the box, a NI-board (National Instruments 6229) was placed which communicated via a NI-cable to the xPC real-time computer (University of Twente). This computer communicated via an ethernet cable with a Thinkpad T440 (Lenovo) on which Simulink 8.4 MATLAB R2014 (Mathworks) ran. Besides, the EMG Trigno System was connected to the xPC and laptop as well.

D. Control laws

In this section the parameters for the control laws are explained.

1) No control (NC): In this case, only the passive balancing mechanism was used. The motor was not enabled, mimicking the passive device.

2) Standard admittance (SADM): In this case, standard admittance was added to control the motor output. The standard formula for admittance is:

$$H = \frac{1}{ms^2 + bs + k} \tag{1}$$

Where m is the virtual inertia, b is the virtual damping and k is the virtual stiffness.

The values for the parameters were tuned manually with the help of a pilot subject. The values were fixed for all subjects, similar to Lenthe et al. [11]. In Table I the values of the parameters are depicted. The stiffness k was set to zero. It was unwanted to have an extra spring effect when the subject moved further from the neutral position, this was already present because of the passive device.

The input of the standard admittance was normalised and limited, therefore maximum input only costed subjects 50% of the maximum force determined at the beginning of the experiment. More detailed information is given in Appendix A.

TABLE I: Parameters for control laws

Parameter	Standard admittance	Variable admittance
m	0.15	acc: $\frac{M_f B_v}{B_f}$ dec: $\frac{M_f(B_f - \alpha_a \lvert\ddot{\theta}\rvert)}{B_f}$
b	0.7	acc: $B_f - \alpha_a \lvert\ddot{\theta}\rvert$ dec: $B_f + \alpha_d \lvert\ddot{\theta}\rvert$
k	0	0

3) Variable admittance (VADM): For the case study, a third condition was added; variable admittance control. From [11] and [16], it was shown that this admittance is promising in reducing movement time compared to standard admittance control. Therefore it was decided to include this control law in the experiment as well. The variable admittance had different parameter values depending on the event (acceleration or deceleration of the head of the subject in flexion and extension direction) which was recognized by the control law.

Two intentions were identified during the experiment, either acceleration or deceleration of the head of the subject. When acceleration was detected, the inertia and damping values both decreased. For deceleration, the inertia value decreased as well, but the damping value increased. All values changed in proportion to the magnitude of the deceleration/acceleration ($\alpha_a|\ddot{\theta}|$). In Table I the values are depicted. M_f and B_f are the standard parameters with respectively values of 0.15 and 0.7. B_v is the current damping value and α_a and α_d are the change-ratio's (see Appendix A.6). Events are detected by comparing the signs of velocity and acceleration of the device. If the signs are equal, there is acceleration, if they do not match, the intention is deceleration [11], [16].

E. Task

In literature, two tasks are mainly used to evaluate the performance of admittance controllers. Both tasks are tracking tasks, one of them is a continuous tracking task [14], [17], [18] and the other is a discrete position tracking task [11]–[13], [19]. During the continuous tracking task, subjects are asked to follow a target as closely as possible. For the discrete position tracking task, subjects are asked to move as fast and accurate as possible to a fixed point. This task is also called a Fitts' like experiment, because it uses the principles of Fitts' law [20]. To be able to compare the results of this experiment to the experiment of Lenthe et al. [11], in which they compared standard and variable admittance control for an actuated trunk device, it was decided to use a Fitts' like experiment. From literature it is known that Fitts' law also holds for head movements [21], [22]. And with this experiment, we can investigate whether Fitts' law holds for our control law as well.

In Appendix B it is calculated that this kind of experiment can be performed with this motor and device. Fitts' law tells us that the relation between the index of difficulty of a target

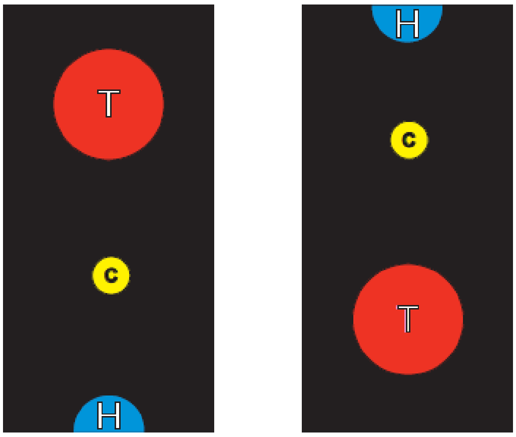

Fig. 2: User interface of the experiment, the red, yellow and blue dots respectively represent the target (T), subject angle (c) and home position (H). [11]

and the movement time is constant [20]. The formula, when Fitts' law holds, is:

$$MT = a + b \cdot ID \tag{2}$$

Where MT is the movement time to the target, a and b are parameters depending on the environment and ID is the index of difficulty. In Lenthe et al. [11], they do not use Fitts determination of the index of difficulty, but that of MacKenzie [23], which uses the logic of Shannon's Theorem 17 [24]:

$$ID(bits) = log_2(\frac{A}{W} + 1) \tag{3}$$

Where D is the distance in pixels from the home position to the target and W is the target width in pixels. The difference between Fitts' equation and that of MacKenzie is small, but MacKenzie's model showed a slightly higher r-value, which implicates a better strength of a linear relationship [23]. This and the fact that Lenthe et al. [11] used MacKenzie's model were the deciding factors to use MacKenzie's model in this paper.

In total, six targets were used in the experiment. The ID's were calculated using Equation 3. *W* had a fixed width of 100 pixels. For every direction (flexion and extension) three targets with ID's of 3, 4 and 5 were used. In Table II the target's pixel distance and corresponding angle are displayed.

In this experiment, the task was performed virtually, on a screen (1680x1050 pixels). Rotation of the head in the sagittal plane corresponded to moving a cursor up and down a screen. The subject had to move their head from -12 (extension) to

TABLE II: Target specifications. The angle is given for the flexion and extension direction.

ID (bits)		3	4	5
Pixel distance		396	792	1584
Angle (deg)	F	-3.9	+4.2	+20.4
	E	+13.9	+5.8	-10.4

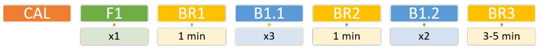

Fig. 3: Experiment flow for one condition, this flow was repeated for the amount of conditions the subject performed. CAL1 is the calibration phase, where also the maximum force and force compensation were included. F1 is the familiarization block, B1.1 and B1.2 are the main blocks, BR1 and BR2 were short breaks of approximately 1 minute, depending on the subject. BR3 was a longer break between the control laws, where the headband was taken off to give the subjects some release of pressure. This break was approximately 3-5 minutes.

+22 (flexion) degrees at maximum. These values were chosen in such a way that the subject could still see the screen when he/she was in the maximum position. The interface, which was projected on the screen, looked like Figure 2. The yellow circle represented the head angle of the subject (cursor).

The subjects were first asked to keep the cursor on the home position (blue target). This target appeared either on the top or bottom of the screen, respectively corresponding to approximately 12 degrees of extension or 22 degrees of flexion of the head. The subjects needed to keep the cursor still for a random time (1-4 seconds) and when they were successful, a red target was displayed to which the participant should move as fast as possible. This was successful if they stayed in the target for 2 seconds (dwell time).

F. Experimental protocol

Before the start of the experiment, the subjects received an information letter (see Appendix D). They filled in an informed consent (see Appendix E) and demographics (Appendix F). Before they were placed in the wheelchair, the electrodes were placed (for more information see Section II-G). In Appendix G the whole experimental protocol can be seen.

After being seated in the wheelchair, the head support was adjusted and attached to the head of the subject. Each subject performed a maximum force (MF) in flexion and extension direction. This maximum force was used to normalize the input force for the admittance control (see Appendix A.5). After this MF phase, the force was measured along the path from -13 to 25 degrees, while the subject was asked to relax completely. In this phase, the internal and external forces were measured and used as force compensation to be sure no force was measured when the subject was completely relaxed (for more detailed information see Appendix A). This MF phase and the force compensation phase were repeated before each condition.

For the main experiment two conditions were used (two sets of trials). The sequence of the conditions was randomized using Excel, to rule out learning effects. For the case study with two subjects, three sets of trials were done, including also VADM. Here, the first two conditions were randomized, and the third condition always was the VADM.

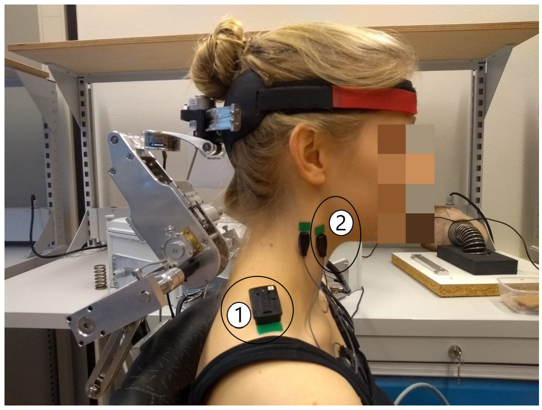

Fig. 4: Sensor placement on one of the subjects. No. 1 is the sensor on the right upper trapezius, and no. 2 is the sensor on the right sternocleidomastoid. The sensor which is not labelled, was not used in this experiment.

Every set of trials was split up in three blocks. In the first block (familiarization) consisting of three times three randomized targets in two directions (1x18 trials), the subject practised with the condition (Appendix C.6). The second and third block, consisting of respectively 3 x 18 and 2 x 18 trials, were used for data analysis. Between the blocks, a break was taken of approximately 1 minute. At the end of the set of trials a longer break was included, while the data of the set of trials was saved. This took approximately 3 to 5 minutes. In Figure 3, a flowchart for one set of trials is depicted.

After the experiment, the subjects were asked to fill out a questionnaire (see Appendix F)

G. Electromyography

To determine if the admittance controller decreased muscle activity, muscle activity was measured with surface electrodes, TRIGNO^{TM} Wireless System (Delsys). One wireless sensor consist of two electrodes. The activity of two muscles, the upper trapezius (UT) and sternocleidomastoid (SCM) was measured. Four sensors were used for this experiment, two for the UT (left and right) and two for the SCM (left and right), see Figure 4. This was in accordance to what Mahmood et al. [9] measured in their passive head support experiment. The sensor location for the UT was chosen following the method of [25]. For the SCM, the sensor was placed at one third of the muscle from the mastoid process to the collar bone. The sensor location was cleaned with alcohol and, if needed, shaven. Before starting the experiment, it was checked whether the sensors showed sufficient signal by performing head rotations and shoulder raising.

H. Data processing and analysis

All data was sampled at 1 kHz via the real-time xPC. The data was then analysed in MATLAB R2019b. Performance of the control law was evaluated by movement time, overshoot, Fitts' law and muscle activity.

TABLE III: Statistical testing: p-values for EMG activity, Movement Time (MT) & Overshoot per ID and direction

			Flexion			Extension		
Parameter	Test		3	4	5	3	4	5
EMG	Sign Test	UT	1.000	0.289	1.000	0.727	0.727	0.727
EMG	Sign Test	SCM	0.727	0.727	0.727	0.727	0.289	0.289
MT	Paired t-test	N/A	**0.006**	**0.000**	**0.003**	**0.000**	**0.008**	**0.001**
Overshoot	Wilcoxon Signed Rank Test	N/A	0.149	**0.021**	**0.018**	**0.012**	**0.036**	**0.017**

1) Movement time: Performance of the control law was evaluated using movement time (MT). Movement time was defined as the time when the target appeared until the subject reached the target, excluding dwell time and reaction time. Dwell time was constant for every subject and target (2s). The reaction time was defined as the time, when subjects moved at least 0.75 degrees from the beginning of the trial. Other articles used a percentage of the maximum speed [11], [26], however, due to noise of the potentiometer, it was not possible in all trials to determine the speed of the subject's head using this percentage. It was, therefore, decided to take a minimal distance which could be detected outside the noise.

The movement times were separated per target ID and direction. Per subject and ID-direction combination, 15 trials were obtained from the second and third block. For performance evaluation the average movement time per subject per ID-direction combination has been looked at. The data was paired, because every subject performed the experiment for both conditions.

2) Overshoot: A trial was successful when the subject held the target still for at least 2s (dwell time). However, it was possible that the subject reached the target and then went out of the target range, this we called overshoot. The amount of overshoot said something about the stability of the movement and was used as a performance indicator. For every trial the times overshoot occurred was counted. This was separated per ID and direction, obtaining 15 data points per subject for one ID-direction combination. To compare between subjects an average per subject was calculated.

3) Fitts' law: Fitts' law states that there is a linear relation between the ID of the target and the movement time. A linear regression fit was determined through the average ID-direction movement times of the subjects to see if Fitts' law could be applied. The linear regression coefficients and the parameters of the fit for standard admittance and no control are compared with each other and literature.

4) Muscle activity: EMG was collected and filtered using a bandpass second order butter filter of 10-400 Hz and a high pass filter (30 Hz) to filter out ECG contamination and movement artefacts [27]. A bandstop filter (49 - 51 Hz) was used to filter out hum from the mains electricity. Two bandstop filters (295-297 and 370-371 Hz) were used to filter out unwanted high peaks which were visible in the power spectrum of the EMG at the same frequency for all subjects. The EMG data was rectified and a moving average filter with a window of 300 ms [28] was used.

Muscle activity was also used as a parameter to test the performance of the control law. In Mahmood et al. [9], they looked at the muscle activity at certain static angles. However, for this experiment it was more interesting to see what the muscle activity was during the movement, because the control laws were only active during the movement. Therefore, the average EMG amplitude during the movement was looked at. Data was separated per target ID and per direction, resulting in 15 data points per subject for every target-direction combination. The value of the left and right electrode of the muscle was averaged, assuming symmetry in the human body (for the flexion-extension direction).

The processed EMG data was not normalised (see Appendix C.3) as no MVC had been performed. It was, therefore, not possible to compare the results between subjects. However, within a subject, EMG configuration was not changed between conditions. Therefore muscle activity difference, lower or higher activity of the passive device compared to the standard admittance, was calculated per subject.

5) Statistics: All statistical analyses were performed within IBM SPSS Statistics 25. Normality was tested with the Shapiro-Wilk Test (small sample size). All data was paired, so if the data was normally distributed a paired t-test was used, otherwise a Wilcoxon signed rank test was used. For the muscle activity a sign test was used as amplitude difference cannot be compared between subjects because no normalisation was done. Therefore the sign test was more appropriate.

For all tests a p value < 0.05 was assumed significant.

III. RESULTS

A. Movement Time

In Figure 5 the average movement time per ID, per direction and per control law is displayed. The data is displayed in box plots. Every box plot represents the averaged data for eight subjects. For each subject, an average movement time was calculated per ID and direction. The paired t-test showed that there was a significant evidence of an increased movement time for standard admittance ($p<0.05$) for all ID's in both flexion and extension direction. These differences are marked by an asterisk. In Table III the results from the t-test are depicted (MT). It can also be seen from Figure 5 that the variance of the movement time for SADM was higher than that of NC.

Subject 6 and 8 performed an extended experiment (case study). These results are depicted in Figure 7 and Figure C.4 (Appendix C.2.2) respectively the results of subject 8 and 6.

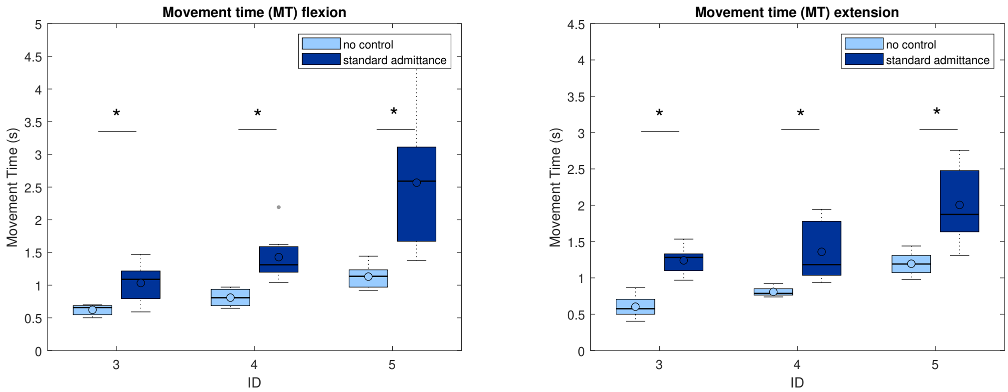

Fig. 5: Mean movement time (MT) for all subjects (n = 8) per direction for all target ID's per control law are displayed. Every box plot represents 8 average MTs per subject. The asterisk marks a p-value < 0.05 according to the Paired T-Test.

For these box plots, each box plot represent 15 trials (separated per ID, direction and control law). For both subjects, for the extension direction, it could be said that a trend was seen for an increased movement time for VADM compared to NC and SADM for ID 4 and 5. However, for the flexion direction, this trend was not there. Besides, for subject 6, VADM showed a big difference compared to NC and SADM for flexion ID 5.

B. Overshoot

The bar graphs in Figure 6 show the amount of times overshoot occurred during one movement. The mean over all trials per ID was taken for each subject and used in this figure. The bar represents the mean over all subjects. Not all data was normally distributed, therefore a Wilcoxon Signed Ranked Test was done to see if there were any significant differences (see Table III). For all targets, except ID 3 flexion, a significant difference was seen in the amount of overshoot. For all significant differences, SADM had a higher amount of overshoots than NC. Looking more closely at the data for this overshoot, it was seen that there were also some high numbers present in the data (counts of 30, 27, 26 etc.).

For the case study (subject 6 and 8) results are depicted in Figure C.7 in Appendix C.4. No consistent trend could be seen for both subjects.

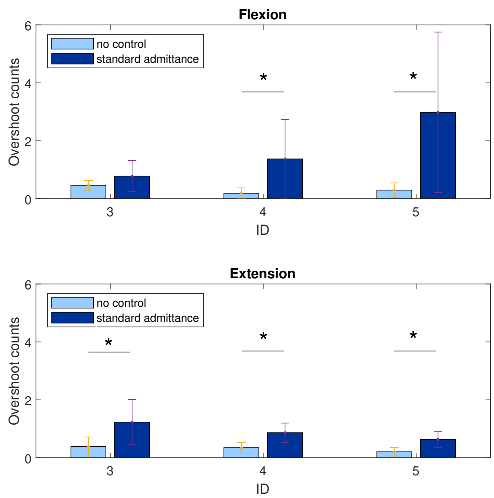

Fig. 6: Amount of overshoots per ID and direction. The mean over all subjects (n=8) was taken. The error bars represent the standard deviation. Significant differences are indicated with an asterisk ($p<0.05$) according to the Wilcoxon test.

C. Fitts' law

In Figure 8 the linear regression lines for all directions and control laws are depicted. This line was based on the average movement time of the subjects per ID. In Figure 8a, b, d and e the lines are separated per direction and control law and in Figure 8c and f the lines are displayed per movement direction. In Table IV the regression parameters are noted. Parameter b is the slope of the line in seconds/bits and parameter a is the offset of the slope. R represents the regression coefficient, the squared of this value (R^2) tells us how much of the variance of the data points can be explained by the regression fit. For both flexion and extension, the R (regression coefficient) was the lowest in the standard admittance control law. Besides, R^2 was less than 0.5 for SADM in both directions. As seen in Figure 8c, the slope of standard admittance is steeper than that of no control and from Figure 8f it can be seen that the offset of standard admittance is higher than no control.

In Figure 9 the residuals plots are depicted. The residuals are plotted against the ID values. It can be seen that there is

TABLE IV: Linear regression parameters

Flexion

Control law	b[s/bits]	a[s]	R	R^2
NC	0.2425	0.2622	0.76776	0.58946
SADM	0.7585	-1.2153	0.69229	0.47927

Extension

Control law	b[s/bits]	a[s]	R	R^2
NC	0.2677	0.1735	0.83602	0.69893
SADM	0.3535	0.5289	0.54003	0.29163

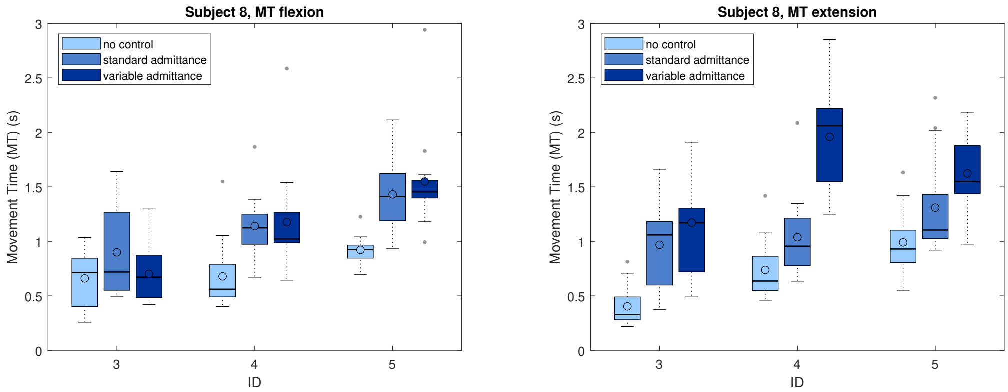

Fig. 7: Movement time (MT) for one subject (subject 8) per direction for all target ID's and control laws. Every box plot represents 15 MTs, which are all MTs per trial (without familiarization).

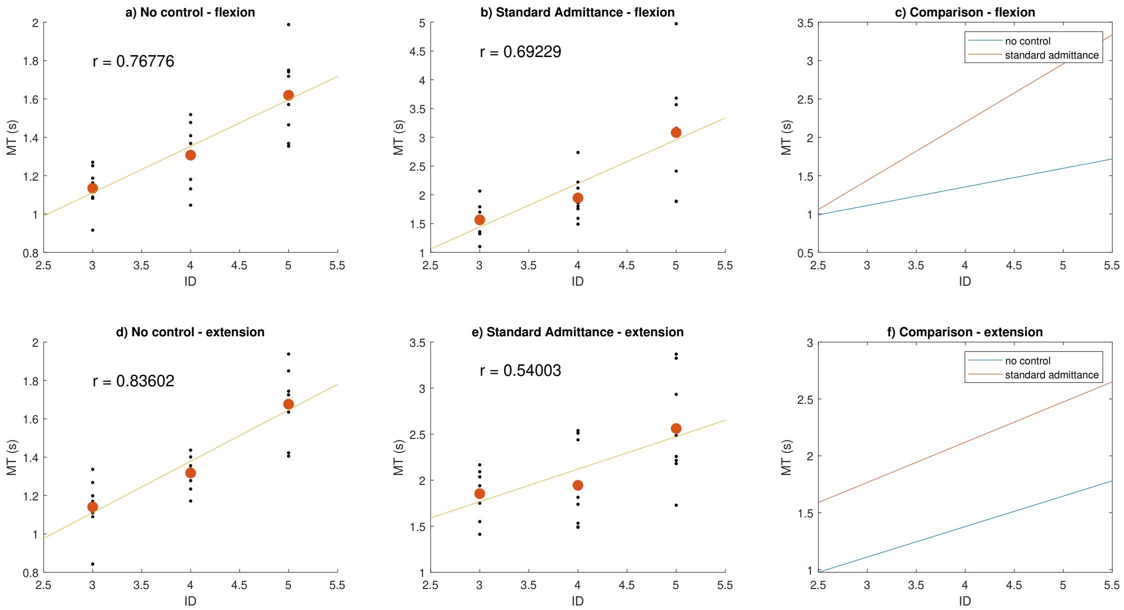

Fig. 8: A linear line was plotted through all the subject data points for the movement time. In a) and d) NC is represented, in b) and e) SADM is represented and both their lines can be seen in c) and f).

more variance in MTs for SADM than for NC. Besides, for the extension direction, for both control laws, a slight shift of points above the zero line is visible for ID 4. This is also the case for SADM flexion for ID 4.

D. Muscle activity

To compare the results of the muscle activity of the main experiment within the subjects, a sign test was performed. This comparison was per subject, per muscle (average left and right), target ID and direction, meaning that the electrode voltages within the subjects were compared. The results of the difference test for all subjects are displayed in Figure 10. Every bar graph represents the amount of times that either the standard admittance (SADM) or the no control (NC) electrode voltage was higher than the other. The results from the sign test in SPSS are displayed in Table III. There was no significant difference according to the Sign test in any of the ID-direction combinations. For UT flexion and extension and for SCM flexion it differed per target if NC or SADM had a higher activity. For SCM it was most of the time NC that gave a higher muscle activity. In Appendix C.1, in Figure C.1 en Figure C.2 the muscle activities (mV) per subject are plotted. There it is also visible that subject 1 had a lot more variability in her/his EMG activity for UT than the other subjects.

The results for the case study (subject 6 and 8) are depicted in Figure 11, for subject 8, and Figure C.3, for subject 6

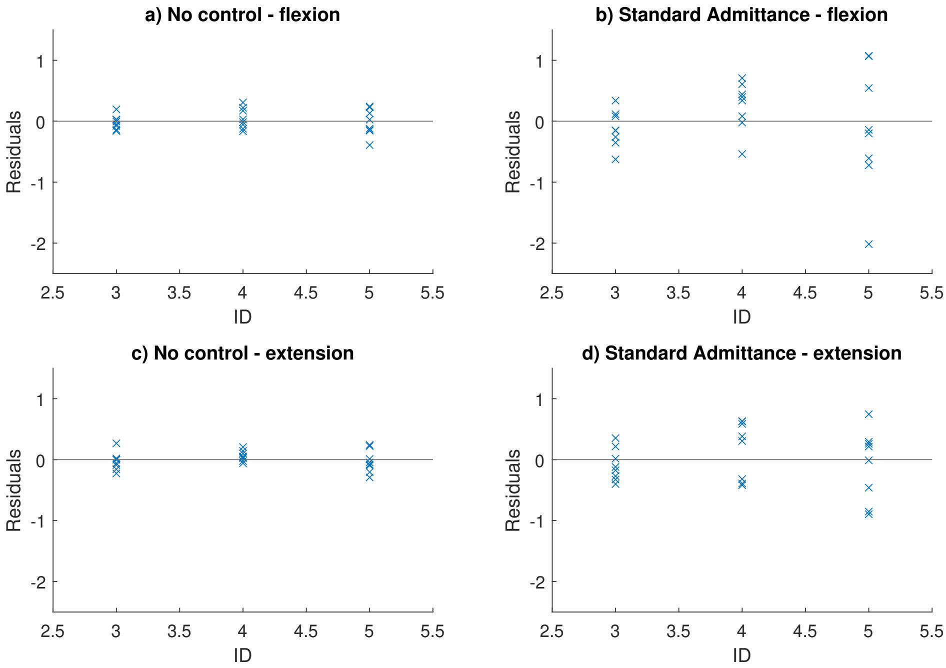

Fig. 9: The residuals of the fitted line from Figure 8 are plotted against the ID values. In Figures a) and b), the results for the flexion direction are depicted for respectively NC and SADM. In c) and d) the results for extension are depicted.

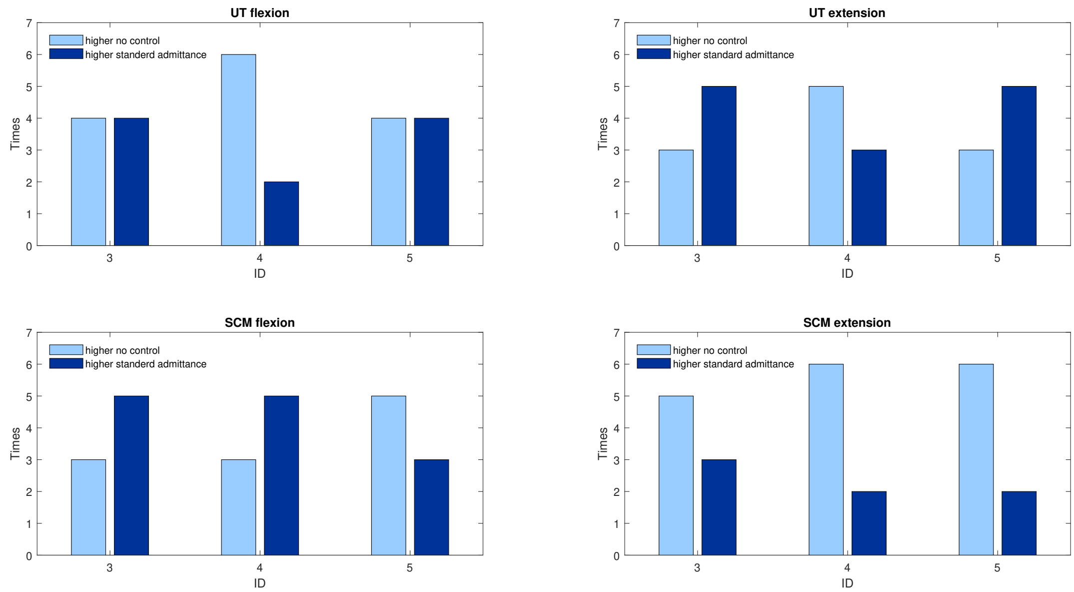

Fig. 10: The bar graphs represent the amount of times that either for SADM or NC the electrode voltage was higher than the other control law within a subject. The results of all subjects (n=8) are displayed.

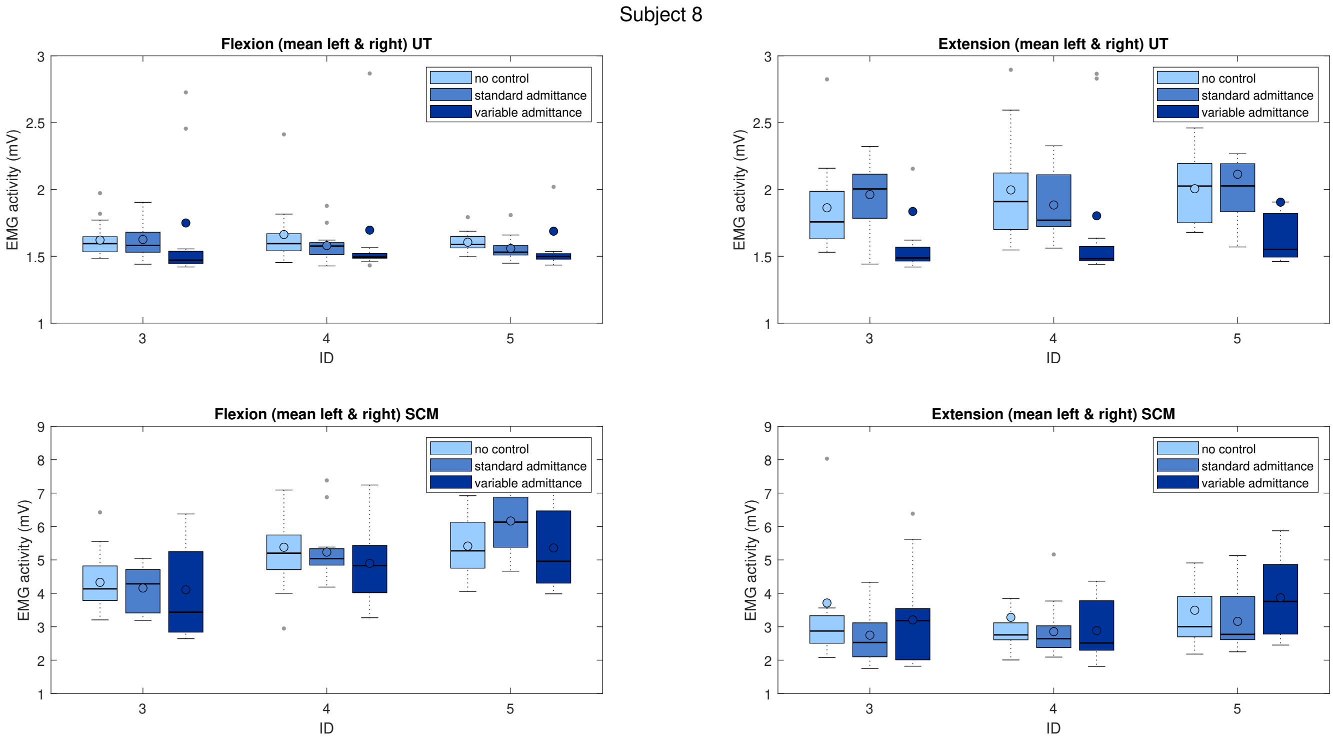

Fig. 11: Muscle activity (mV) for one subject (subject 8), per muscle, per direction, per target ID, per control law. The box plots (+ outliers) represent each 15 trials. The data points were averaged electrode voltages between the left and right side of the subject.

(Appendix C.2.1). For subject 8 (Figure 11) a decreasing trend was only seen for the VADM in UT extension and flexion compared to SADM and NC, when outliers were not taken into account. For SCM flexion, the values of VADM are slightly lower than those of the other control laws. For SCM extension it differed per target. For subject 6 (Figure B.3), an increasing trend was seen in both directions for SCM for VADM compared to NC and SADM. For the UT it differed per target in both directions.

E. Questionnaire

All subjects (n=8) answered the questionnaire. On the question *"Which control law was easier?"*, all subjects answered NC. Every subject also answered SADM in the question *"Which control law was more tiring"*.

On the question *"Did you think the control law was helping/neutral/resisting"*, 81% said that NC was neutral and 19% thought it was helping. For SADM, 81% answered that the control law was resisting and 19% thought it was helping.

For the case study, both subjects answered that SADM was easier than VADM, but they differed in opinion for the question which was more tiring. Subject 6 thought it was VADM and subject 8 found SADM more tiring. Subject 6 thought that SADM was helping and experienced that VADM was resisting. And subject 8 found SADM resisting and VADM both helping and resisting.

IV. DISCUSSION

The goal of this experiment was to see if the designed standard admittance controller is a successful addition to the passive head support. It was hypothesised that for a Fitts' like experiment, the movement time and the average muscle activity of the subjects would decrease. Besides, the overshoot count would not significantly differ for SADM compared to NC. At last, it was expected that Fitts' law would hold for SADM. For the case study, it was hypothesised that the movement time and muscle activity would even further decrease for VADM compared to SADM.

1) Main experiment (NC vs SADM): From the results it can be concluded that the movement time for SADM has increased with respect to NC. Besides, the overshoot count showed that SADM was less stable compared to NC. Furthermore, there is a small indication that subjects behave according to Fitts' law when connected to the device with SADM. For muscle activity no significant differences were seen and therefore no conclusion on a decrease or increase of the muscle activity can be made. These results were not all in line with the hypothesis.

In literature no direct comparisons between passive devices and admittance controlled devices have been made. However, admittance control has been researched previously for other human segments than the head [11], [12], [14], [15]. Admittance is evaluated with simulations, stability and robustness in Aguirre-Ollinger et al. [15], by tracking error, crossover frequency and information transmission rate by Lobo-Prat et al. (2014) [14]. In Lobo-Prat et al. (2016) [12] they based performance on task completion rate, efficiency, overshoot and smoothness. And in Lenthe et al. [11] admittance performance is expressed in movement time and Fitts' law. The latter experiment is most comparable with our research. However, direct comparison of movement time is not possible because absolute angle differed and another human segment is used.

For comparing the results of Fitts' law to the literature, one needs to look at the parameters (*a*, *b*, R) which were estimated. Parameters *a* and *b* are depending on the experimental conditions [29] and those cannot be compared to the literature, as no comparable experiment has been performed. However, it can be seen that the slope of the SADM is higher than that of NC for the flexion direction. The inverse of the slope is a measure for the information-processing rate of the subjects [30]. From the results it can be said that this rate is lower when subjects are connected to the device with SADM than connected to the passive device, indicating that it is harder for subjects to reach the target with the SADM.

For the regression coefficient, comparisons can be made with respect to literature. In Radwin et al. [22] and Jagacinsky et al. [21] they found r-values of respectively 0.93 and 0.97 for head movements in free space. The values for the NC are lower than those presented in these two articles. In Lenthe, et al. [11] values were 0.82 and 0.87 for SADM. The values for SADM in this article are lower than that of [11], indicating that the subjects were not able to move as optimally as in [11].

When looking at r-values from articles involving Fitts' law, which are less comparable to this paper, values of 0.75 till 0.99 are calculated [19], [26], [31], [32]. The r-value for NC falls in this range, but that of SADM is lower. Besides, r^2 was less than 0.5 for SADM, indicating that less than 50% can be explained by the linear fit.

Low r-values can indicate a bad fit, however, when looking at the residuals plot (Figure 9), it seems that the lower r-value of the SADM can be explained by the bigger variance in the subjects. Meaning the low r-value does not indicate a bad fit, but only a big variance. However, for ID 4 the residuals are shifted a bit above the zero line, indicating that maybe the linear relation from Fitts' law is not the best fit. In conclusion, the low r-values could be due to more variance in the subjects, the small group size, or that the device limits the subjects to move optimally.

In this article, muscle activity is also used as a parameter to compare SADM with NC. For Mahmood et al. [9] muscle activity was decreased, when users had help of the passive head support. However, when looking at the muscle activity in this experiment, no significant difference was visible between NC and SADM. This suggests, that SADM control did not improve the device in this sense, but it also did not worsen it. As can be seen in Appendix C.15, for some subjects the slope of the movement was higher for NC than for SADM, indicating a higher speed. This higher slope could have influenced the muscle activity, as higher speed is positively correlated with a higher amplitude [33].

Regarding the movement time, it could be seen that the movement time for the subjects was significantly higher for the SADM than for the NC. These results suggest that the SADM control law did not provide a benefit for the movement time and the use of SADM in the head support did not help the users. When looking at the overshoot, even more proof for this negative benefit has been shown. There was a significant increase in the times overshoot occurred compared to the NC law. Meaning, the standard admittance control law was less stable, compared to NC.

However, when looking more precisely at the overshoot individual results, it was seen that the amount of times overshoot occurs was very high. Sometimes it even occurred 30 times. When we look closer to this results, we see that a lot of the overshoots had happened because of high noise (Appendix C.5). Because of this noise in the potentiometer, the cursor went in and out of the target when close to the target borders. Therefore, it can be assumed that Figure 6 shows biased results due to the stability of the potentiometer, when the motor was enabled. Because of this, it is harder to get an insight in the performance of the control law from this figure. It was also visible that more overshoot occurred for the flexion direction compared to the extension direction. When relating the noise in the potentiometer to the motor, this makes sense, as in the flexion direction the device was further away from the neutral position. At this point, the motor had a higher voltage input, resulting in more vibrations of the motor, which resulted in more noise as well. However, it is not completely certain that the increase of overshoot was only due to noise in the potentiometer. Other factors, such as delay or damping values could have influenced this as well. New experiments, with less noisy sensors, should clarify this.

Figure 6 does also help to explain the increased movement time for the SADM (Figure 5). Because the movement time kept increasing when the dwell time was not reached, going in the target and e.g. staying there for 1.8s before going out was calculated as movement time and not as dwell time. Therefore, the instability of the potentiometer could also influenced have the higher movement time for SADM.

Looking at the regression coefficients, it is possible that the linear line through the data points was affected as well by the noisy potentiometer. Therefore, it could be possible that Fitts' law also holds better for the SADM control law when a stable cursor was used. This should be investigated in the future.

The current outcomes were all in line with the answers of the subjects on the questions *"Which control law was easier?"* and *"Which control law was more tiring?"*. Every subject answered that NC was easier and SADM was more tiring, which could be explained by the fact that the potentiometer caused difficulties in getting the cursor stable on the target. However, other factors such as system delay could have influenced these results as well.

To see if decreasing the dwell time would help with the high amounts of overshoot, one should look at Appendix C.7. The results show that with a decreased dwell time, the amount of overshoot decreases as well. The noise still influences this amount and overshoot is therefore still biased, however less. It is also seen that with a decreased dwell time, the movement time is still significantly higher for SADM than for NC. Therefore, some part of it could be due to the noise, but delay in the system is also something which could have caused the longer movement time.

Taking all the above mentioned discussions into account, it is therefore not recommended to use this standard admittance control with the current experimental set-up.

2) Case study (VADM vs SADM/NC): For the case study, it seemed that the movement time increased even more for the VADM in the extension direction. This was also in line with the answers on the questionnaire. Both subjects answered that SADM was easier than VADM. This suggests that VADM was not a better control law than SADM. Unfortunately, this was not as expected in the hypothesis. However, for the flexion direction MT did not increase. Furthermore, if you look at the muscle activity, Figure 11 and Figure C.3, no conclusions can be made, as both subjects showed contradictory results. In Lenthe, et al. [11] a clear decrease in movement time was seen for VADM, which was not applicable here. An explanation could be that other damping-inertia ratio's are used. Another reason could be that the subjects were more tired, both subjects performed this control law as the third condition, asking a lot of the subjects attention already in the first two conditions.

A surprising thing which is visible in Figure 11 (subject 8), is that for the UT, the mean of the muscle activity data points was higher than the box plot and median. This was due to some outliers which were also taken into consideration calculating the mean. These outliers were present only for the right UT electrode in the repetitions after the short break. These outliers might have been caused by voluntary movements of the right arm of the subject. If these outliers were taken out, the VADM average would be lower than that of SADM and NC, which would suggest that subject 8 had a decreasing muscle activity. However, these results were not seen for subject 6, therefore no hard conclusion can be made on whether the VADM was a better control law than SADM.

Regarding Fitts' law, no comparisons have been made, because only two subjects did the experiment. More research allows for comparison of the regression coefficient for VADM.

3) Limitations of the experimental set-up: As mentioned earlier, the potentiometer had a lot of noise when the motor was turned on. It would be recommended to work with the encoder of the motor, because this encoder does not show noise from the motor itself. Unfortunately in this set-up using the encoder was not a possibility, because slip occurred between the motor and the device. This was noticeable because the difference between the position, determined via the potentiometer and the encoder, seemed to vary a lot. The encoder, therefore, was not a reliable source for the position of the head. Another unwanted effect of the slip of the motor was that subjects could cause slip of the motor, when they produced a high torque. This happened during the experiment with the standard admittance control and variable admittance control. Potentially during these time, the system was not fully controlled by the SADM control law (or VADM control law in the case study). Redesign of the current set-up is desired, because it might lead to other conclusions.

Another limitation of this study was that no normalised EMG was used (see Appendix C.3). Therefore, comparisons between subjects could not be done.

V. Conclusions and Future Recommendations

Evaluation of a developed standard admittance control law on a active head support was performed. This evaluation was done with the help of a Fitts' like experiment with eight subjects. Besides, a case study with two subjects was performed, to test the performance of a variable admittance control law. The conclusion of this evaluation is that the standard admittance control law, designed as it is with the current set-up, did not decrease movement time and muscle activity and there was only a small indication that Fitts' law holds. However, in the future, experiments with a less noisy position sensor should be done, to test the performance of the control law. VADM showed conflicting results regarding movement time and muscle activity. Research with more participants should be performed, to see if the VADM is a potential control law for the head support. However, this should be done with a less noisy position sensor, as mentioned above.

It is also advised to do a extended MVC determination for the EMG. In this way performance between subjects can be evaluated, giving more insight in the decrease of muscle activity.

It would also be interesting in the future to look at inertia compensation as an addition to admittance control, which has shown promising results in the paper of Aguirre-Ollinger et al. [18].

Acknowledgement

The author would like to thank A.M. Geers for her insights and feedback during the whole process. Besides, thanks are given to M.N. Mahmood, M. Wessels and S. Verros for their help and support. Furthermore, the author would like to thank H.F.J.M. Koopman, A. Bergsma and E.C. Prinsen for being a committee member and for their feedback. The author would also like to thank all the subjects for their time and effort.

REFERENCES

[1] "Over ALS," https://www.als.nl/wat-is-als/, Accessed: 20-05-2019.

[2] "Spinale Musculaire Atrofie (SMA)," https://erfelijkheid.nl/ziektes/spinale-musculaire-atrofie-sma, Accessed: 16-05-2019.

[3] "Wat is Duchenne Spierdystrofie," https://duchenne.nl/wat-is-duchenne-spierdystrofie/, Accessed: 17-05-2019.

[4] N. Yoganandan, F. A. Pintar, J. Zhang, and J. L. Baisden, "Physical properties of the human head: Mass, center of gravity and moment of inertia," *Journal of Biomechanics*, vol. 42, no. 9, pp. 1177 – 1192, 2009. [Online]. Available: http://www.sciencedirect.com/science/article/pii/S0021929009001444

[5] "The headmaster collar," https://www.symmetric-designs.com/headmaster-collar, Accessed: 21-05-2019.

[6] "Necksolutions headrest," https://www.necksolutions.com/wheelchair-headrests/, Accessed: 21-05-2019.

[7] "Focal modular headrest," https://www.focalmeditech.nl/en/modular-headrests, Accessed: 21-05-2019.

[8] M. Jansen, N. van Alfen, A. C. H. Geurts, and I. J. M. de Groot, "Assisted bicycle training delays functional deterioration in boys with duchenne muscular dystrophy: The randomized controlled trial "no use is disuse"," *Neurorehabilitation and Neural Repair*, vol. 27, no. 9, pp. 816–827, 2013, pMID: 23884013. [Online]. Available: https://doi.org/10.1177/1545968313496326

[9] M. Mahmood, A. Tabasi, I. Kingma, and J. van Dieën, "A novel passive neck orthosis for patients with degenerative muscle diseases: Development and evaluation," *Not yet published*, 2019.

[10] K. Anam and A. A. Al-Jumaily, "Active exoskeleton control systems: State of the art," *Procedia Engineering*, vol. 41, pp. 988 – 994, 2012, international Symposium on Robotics and Intelligent Sensors 2012 (IRIS 2012). [Online]. Available: http://www.sciencedirect.com/science/article/pii/S1877705812026732

[11] P. G. Van Lenthe, S. Verros, E. E. G. Hekman, R. Carloni, and H. F. J. M. Koopman, "Comparing assistive admittance control algorithms for a trunk supporting exoskeleton," in *2018 IEEE International Conference on Robotics and Automation (ICRA)*, May 2018, pp. 2828–2834.

[12] J. Lobo Prat, P. Kooren, M. Janssen, A. Keemink, P. Veltink, A. Stienen, and H. Koopman, "Implementation of emg- and force-based control interfaces in active elbow supports for men with duchenne muscular dystrophy: a feasiblitity study," *IEEE transactions on neural systems and rehabilitation engineering*, vol. 24, no. 11, pp. 1179–1190, 11 2016.

[13] J. Lobo-Prat, P. N. Kooren, A. Q. L. Keemink, M. I. Paalman, E. E. G. Hekman, P. H. Veltink, A. H. A. Stienen, and B. F. J. M. Koopman, "Design and control of an experimental active elbow support for adult duchenne muscular dystrophy patients," in *5th IEEE RAS/EMBS International Conference on Biomedical Robotics and Biomechatronics*, Aug 2014, pp. 187–192.

[14] J. Lobo-Prat, A. Keemink, A. Ha Stienen, A. Schouten, P. H Veltink, and B. Hfjm Koopman, "Evaluation of emg, force and joystick as control interfaces for active arm supports," *Journal of neuroengineering and rehabilitation*, vol. 11, p. 68, 04 2014.

[15] G. Aguirre-Ollinger, U. Nagarajan, and A. Goswami, "An admittance shaping controller for exoskeleton assistance of the lower extremities," *Autonomous Robots*, vol. 40, no. 4, pp. 701–728, Apr 2016. [Online]. Available: https://doi.org/10.1007/s10514-015-9490-8

[16] A. Lecours, B. Mayer-St-Onge, and C. Gosselin, "Variable admittance control of a four-degree-of-freedom intelligent assist device," in *2012 IEEE International Conference on Robotics and Automation*, May 2012, pp. 3903–3908.

[17] Y. Zhuang, S. Yao, C. Ma, and R. Song, "Admittance control based on emg-driven musculoskeletal model improves the human–robot synchronization," *IEEE Transactions on Industrial Informatics*, vol. 15, no. 2, pp. 1211–1218, Feb 2019.

[18] G. Aguirre-Ollinger, J. E. Colgate, M. A. Peshkin, and A. Goswami, "Inertia compensation control of a one-degree-of-freedom exoskeleton for lower-limb assistance: Initial experiments," *IEEE Transactions on Neural Systems and Rehabilitation Engineering*, vol. 20, no. 1, pp. 68–77, Jan 2012.

[19] S. Verros, N. Mahmood, L. Peeters, J. Lobo-Prat, A. Bergsma, E. Hekman, G. J. Verkerke, and B. Koopman, "Evaluation of control interfaces for active trunk support," *IEEE Transactions on Neural Systems and Rehabilitation Engineering*, vol. 26, no. 10, pp. 1965–1974, Oct 2018.

[20] P. M. Fitts, "The information capacity of the human motor system in controlling the amplitude of movement." *Journal of Experimental Psychology: General*, vol. 121, no. 3, pp. 262 – 269, 1992.

[21] R. J. Jagacinski and D. L. Monk, "Fitts' law in two dimensions with hand and head movements movements," *Journal of Motor Behavior*, vol. 17, no. 1, pp. 77–95, 1985, pMID: 15140699. [Online]. Available: https://doi.org/10.1080/00222895.1985.10735338

[22] R. G. Radwin, G. C. Vanderheiden, and M.-L. Lin, "A method for evaluating head-controlled computer input devices using fitts' law," *Human Factors*, vol. 32, no. 4, pp. 423–438, 1990, pMID: 2150065. [Online]. Available: https://doi.org/10.1177/001872089003200405

[23] I. S. MacKenzie, "A note on the information-theoretic basis for fitts' law," *Journal of Motor Behavior*, vol. 21, no. 3, pp. 323–330, 1989, pMID: 15136269. [Online]. Available: https://doi.org/10.1080/00222895.1989.10735486

[24] R. W. Soukoreff and I. S. MacKenzie, "Towards a standard for pointing device evaluation, perspectives on 27 years of fitts' law research in hci," *International Journal of Human-Computer Studies*, vol. 61, no. 6, pp. 751 – 789, 2004, fitts' law 50 years later: applications and contributions from human-computer interaction. [Online]. Available: http://www.sciencedirect.com/science/article/pii/S1071581904001016

[25] "Recommendations for sensor locations in shoulder or neck muscles," http://seniam.org/, accessed: 2019-12-28.

[26] A. Q. L. Keemink, R. I. K. Fierkens, J. Lobo-Prat, J. S. F. Schorsch, D. A. Abbink, J. B. J. Smeets, and A. H. A. Stienen, "Using position dependent damping forces around reaching targets for transporting heavy objects: A fitts' law approach," in *2016 6th IEEE International Conference on Biomedical Robotics and Biomechatronics (BioRob)*, June 2016, pp. 1323–1329.

[27] M. Redfern, R. Hughes, and D. Chaffin, "High-pass filtering to remove electrocardiographic interference from torso emg recordings," *Clinical Biomechanics*, vol. 8, no. 1, pp. 44 – 48, 1993. [Online]. Available: http://www.sciencedirect.com/science/article/pii/S0268003305800099

[28] P. Konrad, "The abc of emg," *A practical introduction to kinesiological electromyography*, vol. 1, 01 2005.

[29] M. Takeda, T. Sato, H. Saito, and et al., "Explanation of fitts' law in reaching movement based on human arm dynamics," *Sci Rep*, vol. 9, 2019.

[30] R. J. Jagacinski and J. M. Flach, *Control theory for humans*. Lawrence Erlbaum Associates, Inc.

[31] D. E. Meyer, R. A. Abrams, S. Kornblum, C. E. Wright, and J. E. Keith Smith, "Optimality in human motor performance: Ideal control of rapid aimed movements." *Psychological Review*, vol. 95, no. 3, pp. 340 – 370, 1988.

[32] R. Kerr, "Diving, adaptation, and fitts law," *Journal of Motor Behavior*, vol. 10, no. 4, pp. 255–260, 1978, pMID: 15186987. [Online]. Available: https://doi.org/10.1080/00222895.1978.10735159

[33] T. Masuda, T. Kizuka, J. Y. Zhe, H. Yamada, K. Saitou, T. Sadoyama, and M. Okada, "Influence of contraction force and speed on muscle fiber conduction velocity during dynamic voluntary exercise," *Journal of Electromyography and Kinesiology*, vol. 11, no. 2, pp. 85 – 94, 2001. [Online]. Available: http://www.sciencedirect.com/science/article/pii/S1050641100000481

Chapter 3

General conclusion

In this thesis, it has been researched, if admittance control can be a useful addition to a passive head support. Fitts' like experiments with eight healthy subjects and a standard admittance controller have been performed. Besides, in a case study, variable admittance is investigated with two healthy subjects.

The results from this research indicate that the admittance control law, designed as it is, with the current set-up does not provide extra support for the user. In contrast, users take longer to perform the experiment and experience that it is more exhausting. Besides, variable admittance showed conflicting results in comparison with standard admittance, with regard to the movement time and muscle activity. However, due to some limitations of the study, results may lead to different conclusions when these limitations are solved.

To be able to really say something regarding the addition of an admittance control law, new research with less noisy sensors and with no motor slip should be performed. Without this, it is uncertain whether the unexpected results can be blamed on the admittance control or the limitations of the experimental set-up. Since these results also contradict the results from other assistive devices, for which admittance control showed promising results, it is advised to reinvestigate such an admittance controller without the aforementioned limitations.

Appendices

Appendix A

Simulink model overview

For the experiment, mentioned in the paper, a Simulink model is used. This Simulink model determines the flow of the experiment and drives the motor. In Figure A.1, an overview of the Simulink model is depicted. In the following sections, different parts of the model will be elaborated on.

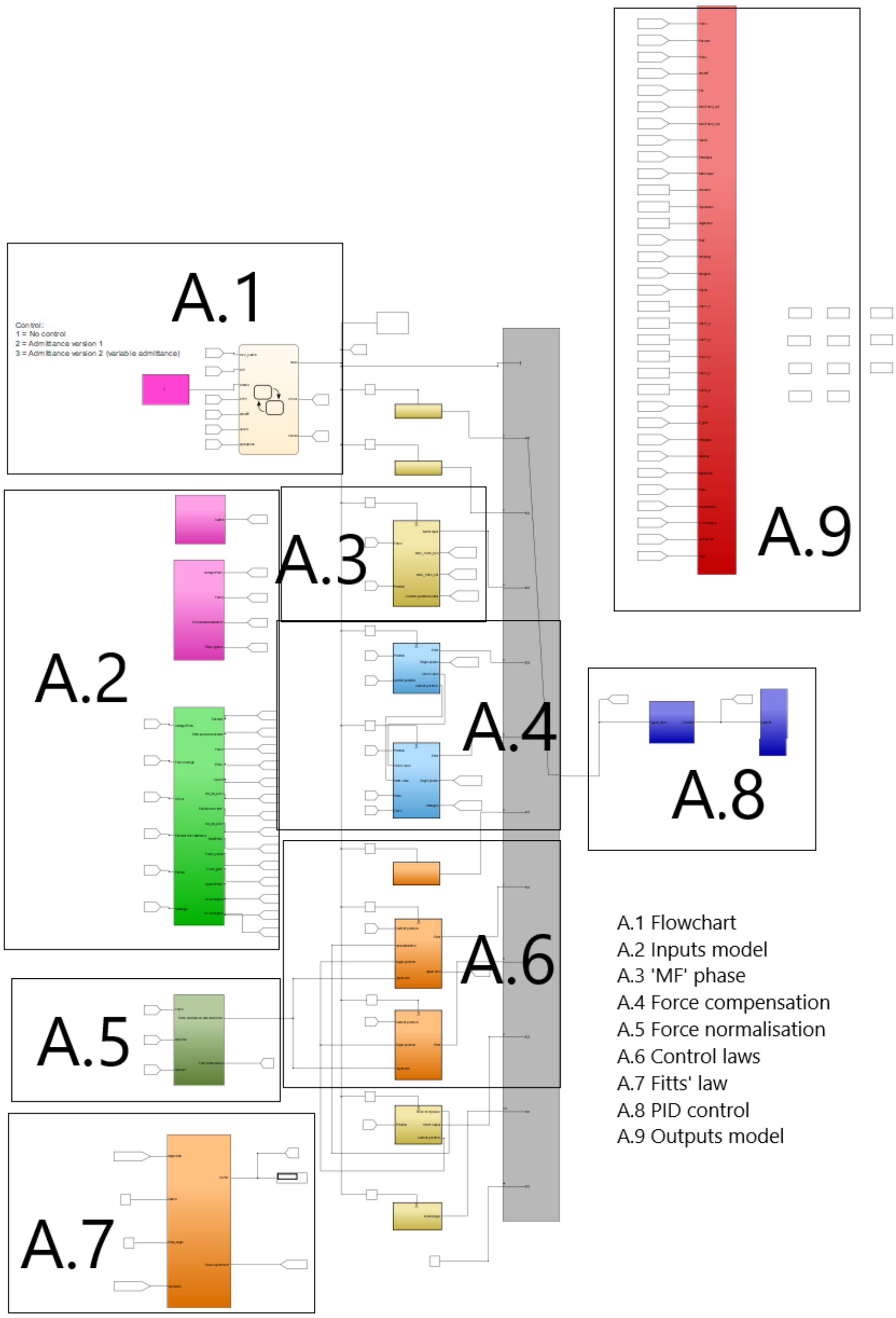

Figure A.1: An overview of the Simulink model, which is used during the experiment explained in the paper, is visualized here.

A.1 Flowchart

Within the flowchart, the steps of the experimental protocol are modelled in Simulink. The flowchart (Figure A.2) has seven inputs, of which two are controlled by the experimenter; 'switch' and 'control' and five are determined inside the model; 'DIP', 'DIP2', 'errorPE', 'speed' and 'speedpodc'. Besides, three variables are outputted; 'state', 'offset' and 'enccal'. The inputs are used in the conditions to go from phase to phase. In Figure A.3, a simplified version of the flowchart is depicted.

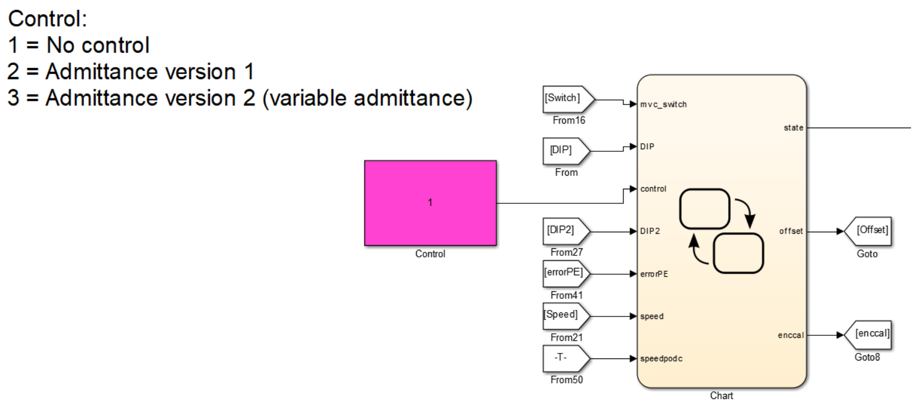

Figure A.2: Part of the Simulink model, zoomed into the chart part.

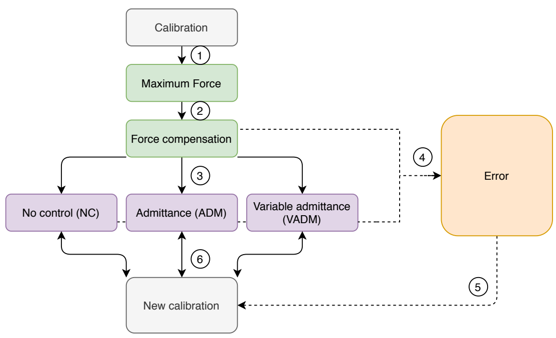

Figure A.3: A simplified version of the flowchart, which is embedded into Figure A.2. In Simulink, conditions are related to the arrows. The most important conditions are marked by numbers and explained in the paragraphs below.

The first block the models goes in is the calibration block. This phase consists of two sensor calibrations. First, the force sensor calibration is performed (output 'offset') and secondly, the encoder calibration (output 'enccal') is done. These calibrations will be elaborated on in respectively Section A.2.2 and Section A.2.3. Going to the next block (no. 1) does not require extra input from the model or user. After a few seconds, the model will automatically go to the next step; the maximum force step.

The second block, in Figure A.3, is the maximum force block. When the model is in this phase, the user is asked to push maximally with the head against the back and the front of the device. In Section A.3, more information on how the maximum force is derived has been described. The condition (no. 2), for going to the next block, requires the switch value to be 1 (see Section A.2.1). This value is changed by the researcher with a manual switch.

The next step is force compensation. This phase consists of two sub phases; extension and flexion of the head. In the extension part, the user will be tilted backwards until the set condition is met. This condition requires the DIP2 value to be smaller than or equal to 0.3. The DIP2 value is the difference between the set end position and the potentiometer value. The end position used for DIP2 is set to -13 degrees. Once the model is in the flexion part, the users head will be brought to the front, until the next condition is satisfied. This condition requires the DIP value to be smaller than or equal to 0.3. The end position value used for DIP is +25 degrees. If the condition is met, the model will go into a 'rest' block, this block is not depicted in the simplified version of the flowchart A.3. Before going to the next block, the switch value needs to be 1 again. Depending on the 'value', which is set before the start of the experiment, the flowchart goes either to the NC, ADM, or VADM block (condition no. 3).

These blocks correspond to the control laws which are used in the experiment (see Section A.6). The model will stay in these blocks until the model is terminated or until error conditions are met.

From Figure A.3, there are two blocks not yet explained; 'error' and 'new calibration'. There are three situations in which the model goes into the error state (condition no. 4). If the model is in the force compensation block, the requirements to go into the error block is: errorPE>=5. The difference between the potentiometer and the encoder is in that case bigger than 5 degrees.

Due to some slip which occurred in the control states: NC, ADM or VADM, using a position error was not feasible. Therefore another condition needs to be satisfied within these states. The new requirements were, speed of the encoder bigger than 120 deg/s or speed of the potentiometer bigger than 125 rad/s. These values are chosen, because the subjects do not got that fast during the experiment voluntarily. If the model is in the error state, the motor is disabled for safety purposes.

There is a possibility to continue the experiment when the model is in the error state. This requires pressing the manual switch button again (condition no. 5). Thereafter, the model goes into the new calibration state. In this state, the encoder calibration is performed once more. To continue the experiment after this, the switch button needs to be pressed again and depending on the control input (condition no. 6), the model will go into that block. Another way to go into the new calibration state is directly from the control blocks, indicated by the double arrows. If the experimenter wants to calibrate in between, he/she can press the switch and calibration process will be started.

A.2 Input Simulink & Processing

The xPC receives 2 different types of input from the National Instruments (NI) board. Digital input, which only consists of zeros and ones, and analog input, which can take on every value. The inputs are 'switch value', 'potentiometer voltage', 'force voltage', 'encoder counts' and 'raw EMG signals'. In the following sections, the processing of every input will be discussed.

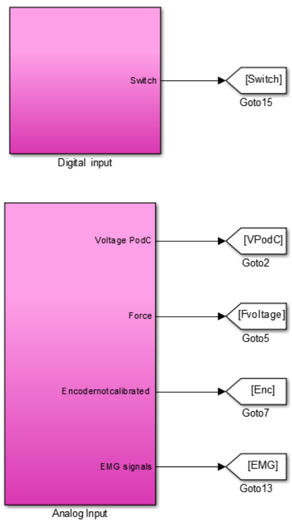

Figure A.4: Part of the Simulink model, zoomed into the inputs part.

A.2.1 Switch

The switch button is connected to the NI-board within the 'electronics' box. This NI-board outputs the signals to the xPC. The value for the switch is a digital input. This value is either zero or one.

When the button is pressed, a value of 1 is given to the xPC, otherwise a value of zero is sent. With this value, the researcher can switch from state to state when this is required.

A.2.2 Potentiometer

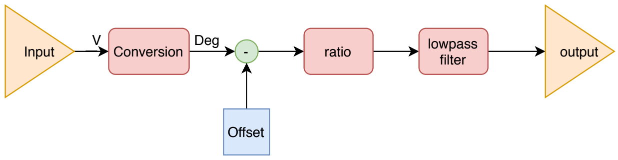

Figure A.5: Flowchart of the processing of the potentiometer.

In Figure A.5, a simplified version of the processing of the potentiometer (Metallux, Conductive plastic hollow shaft sensor PGL 60) is depicted. The potentiometer is also connected to the NI-board, but this signal is an analog input, which can take every value. The input of the potentiometer is a voltage value. This voltage needs to be converted to an angle. To calculate what the voltage-angle relation for this potentiometer is, the following formula is used:

$$\theta = U_{input} * \frac{1}{I * \frac{R_{max}}{\theta_{max}}} \tag{A.1}$$

From the datasheet of the potentiometer, it is known that the potentiometer has an electrical angle (θ_{max}) of 320 degrees and a resistive range (R) of 10kΩ.

$$\frac{R_{max}}{\theta_{max}} = \frac{10 * 10^3}{320} = 31.25 \frac{\Omega}{deg} \tag{A.2}$$

Besides, the maximum voltage which is used is 5V, with this, the current (I) can be calculated.

$$I = \frac{U_{max}}{R_{max}} = \frac{5}{10 * 10^3} = 0.5 * 10^{-3} A \tag{A.3}$$

The input voltage from the potentiometer is therefore divided by the following value for the conversion from volt to angle:

$$I * \frac{R_{max}}{\theta_{max}} = 0.5 * 10^{-3} * 31.25 = 0.015625 \frac{deg}{V} \tag{A.4}$$

After the conversion, an offset is subtracted (see Figure A.5). This offset has a value of 65.20, to set the output to zero when the device is in the neutral position (head angle is zero degrees). Besides, the ratio of the potentiometer to the angle of the head is 2.5, because of the design of the mechanism. Therefore, the angle measured by the potentiometer is divided by 2.5. Thereafter, a Simulink low pass filter with cut-off frequency 10Hz is used to filter out noise in a high frequency.

During the pilot testing it appeared that still a lot of noise was present in the potentiometer signal when the motor was enabled. Therefore, an extra low pass butter worth filter was added with cut-off frequency of 5 Hz.

A.2.3 Encoder

The motor encoder (ENX16 EASY 1024IMP, Maxon Motor) is also connected to the NI-board, and this signal is also an analog input. The input from the encoder is processed before it can be used in the model. In Figure A.6 an overview of this process is depicted. For the conversion of counts into degrees the following formula is used:

$$\theta = counts * \frac{sign * ratio * 360}{CPR * reduction * Quadraturemode} \tag{A.5}$$

The sign is negative, because a negative motor turn is a positive angle change. The ratio from the encoder to the head is 2, because of the design mechanism. CPR (counts per revolution) for this encoder is 1024 (see datasheet motor encoder) and the reduction for the planetary gearhead

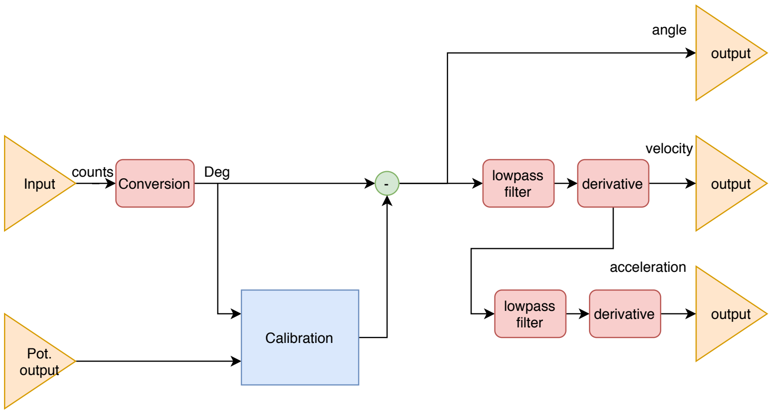

Figure A.6: Flowchart of the processing of the encoder input.

is 243 (see datasheet GPX26HP 243:1). Besides, a quadrature mode of x4 is used. This results in the following value:

$$\theta = counts * \frac{-2 * 360}{1024 * 243 * 4} = counts * -\frac{5}{6912} \tag{A.6}$$

In Figure A.6 a calibration block is also depicted. If the calibration is performed depends on the output of the flowchart. When the variable 'enccal' is 1, the calibration block is enabled, otherwise the calibration block is turned off, keeping the calibration offset on a constant value. When the calibration is enabled, the value of the potentiometer and the encoder are compared for the time duration of the calibration phase and the mean of this value is subtracted from the encoder value. Because of this, the script can be started without having the head support at exactly the zero position.

Besides the angle, it is also interesting to know the speed and acceleration. To get the speed of the encoder, a low pass filter with cut-off frequency 10Hz and a derivative are used, this is repeated to get the acceleration of the encoder.

A.2.4 Force sensor

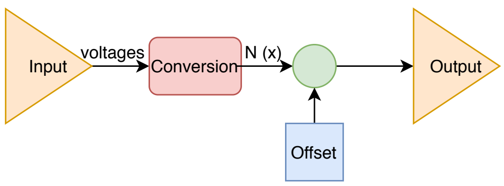

Figure A.7: Flowchart of the processing of the force input.

The force sensor (FT16459) gives an input (analog input) which consist of six values to the xPC. These values need to be calibrated with a sensor specific matrix (FT16459, 'UserAxis'). All input values are multiplied by the calibration matrix and force and moment in x, y and z direction are produced. Only the force in the x-direction is outputted for this model and used for the admittance control. During the calibration, which is activated in the same way as the encoder calibration, the offset of the force sensor is determined. When the calibration phase is over, the offset is held constant. This offset value is subtracted.

A.2.5 EMG

The raw EMG signals of the four electrodes are also analog inputs in Simulink. However, this data is not processed online but it is saved for offline processing in MATLAB R2019b.

A.3 Maximum Force

In this phase, the maximum force produced by the user is saved for normalisation (see Section A.5). In extension direction a maximum negative force is saved and in the flexion direction a maximum positive force is saved.

During this phase, at every sample, the model checks whether the current force is higher or lower than the already saved maximum force. When this is the case, a new maximum force is saved. The current force is an average value of the last 2000 samples, which is acting as an moving average filter, to filter out sudden high forces.

A.4 Force compensation

The force compensation phase consists of two sub phases. In the first phase the head is brought back to a value close to the mechanical end stop (-13 degrees). The devices is rotated with a speed of -0.02 rad/s (-1.15 deg/s). Once this endpoint is reached, the second phase is started.

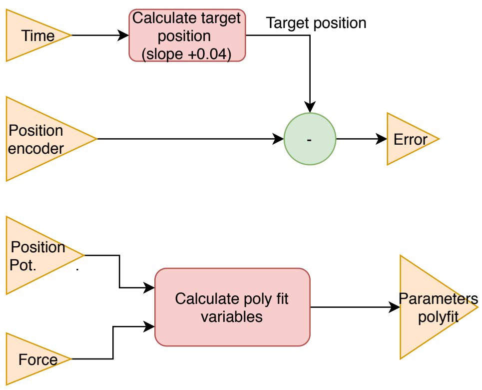

Figure A.8: Flowchart of the second force compensation phase.

In the second phase the real force compensation part starts. In Figure A.8, the simplified version of the second phase is depicted. On the top you can see the flow for the motor movement. The head is brought to the front with a speed of +0.04 rad/s (2.29 deg/s). Every millisecond, a target position is calculated and compared to the current position. This error is going to the PID controller.

When the head is brought to the front, at the same time, the force measured by the force sensor and the position over the movement range (determined by the potentiometer) are saved internally and used for an online polyfit determination with MATLAB. Matlab produces the best fit (third order) for these forces and positions. The parameters for these fit are outputted and used to calibrate the force sensor an extra time (see Figure A.9). In addition to Figure A.7, an extra offset is subtracted. Every millisecond, the model checks which force was measured during the current position (with the fit), and this value is subtracted from the force input.

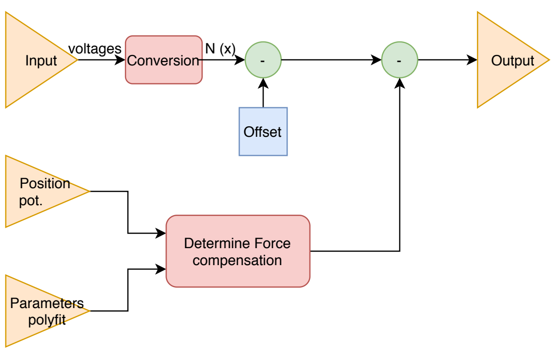

Figure A.9: Flowchart of the processing of the force input with force compensation.

A.5 Normalizing Force

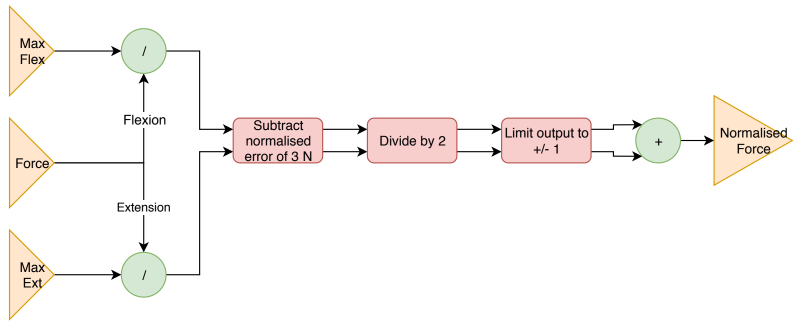

Figure A.10: Flowchart of normalizing and limiting the force input for the control laws.

Before the force is used as input for the control law, it is normalized and limited. Based on the sign of the force, the force is divided by the maximum force in that direction (respectively flexion for negative and extension for positive). During pilot testing it appeared that the force compensation was not exact enough, a normalized error of 3N/maxforce (of extension or flexion) was, therefore, additionally subtracted from the normalized force. Besides, the force was divided by 2. Due to this division, subjects only had to give a force of 50% to get to an input of 1. Therefore, it was necessary to limit the output in such a way that even if 60% is given, the input does not go higher than 1. This normalized and limited force was the input to the control laws, which are explained in the next section.

A.6 Control laws

For the experiment, two or three control laws were used. As mentioned before, the control law input determines, which control law is used during the experiment. Only one control law is used during one model run.

A.6.1 NC

This control law simulates the passive device. The motor is disabled and will not counteract or help the subject.

A.6.2 ADM

With an admittance controller, virtual dynamics with preferred responsive behaviours to a device can be given. For example, a heavy device can appear lighter with the help of an admittance controller. This would be a good solution for people who do not have enough force to move a certain object. In this example, moving the head support can be too energy consuming for people who have trouble in moving their head. With the admittance controller, we want to create a device, which does not need a lot of force to be moving. An admittance controller takes the input force and converts it to a rotational motion. The formula for this is:

$$H = \frac{1}{ms^2 + bs + k} \tag{A.7}$$

The parameters m, b and k can be tuned such that the preferred virtual dynamics are realized. In multiple articles [5–7, 15, 19, 20], this tuning is done manually and with trial and error. With the help of a pilot experiment the preferred combination between the damping b and inertia m was established. The stiffness k parameter was set to 0. There is already a stiffness element in the passive device (the spring) and no further stiffness elements are preferred. The values for b, m and k are respectively 0.7, 0.15 and 0. These values were kept constant for all subjects.

In Figure A.11 the simplified version of the flowchart of the admittance controller is depicted. For the output we want position, which is the double integral of acceleration and rewriting Equation A.7 gives:

$$\ddot{\theta} = \frac{F_{in} - k\theta - b\dot{\theta}}{m} \tag{A.8}$$

This equation is rebuild in the model. The output of the admittance control is compared to the current position and the error between those positions is given to the PID controller.

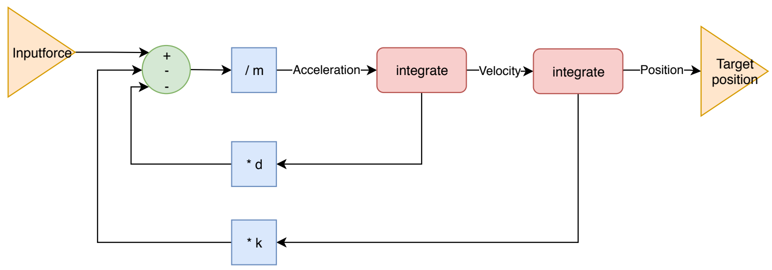

Figure A.11: Simplified flowchart of the admittance control law.

When the device reaches the mechanical endpoints, the acceleration and velocity are set to zero. Even though the subjects still produces force, this measure prevents the motor from producing force when it is not necessary.

A.6.3 VADM

VADM works in principle in the same way as the standard admittance controller. However, the variables change with the direction of the acceleration. So to determine in which direction the acceleration is and to determine the new variables values, a Matlab function is used. This function changes the values of the variables in proportion to the size of the acceleration.

$$b_{acc} = b_f - \alpha_a|\ddot{\theta}| \tag{A.9}$$

$$b_{dec} = b_f - \alpha_d|\ddot{\theta}| \tag{A.10}$$

$$m_{acc} = \frac{m_f b_v}{b_f} \tag{A.11}$$

$$m_{dec} = \frac{m_f(b_f - \alpha_a|\ddot{\theta}|)}{b_f} \tag{A.12}$$

With b_f and m_f the basic values of respectively 0.7 and 0.15 (determined in a pilot experiment) and α_a and α_d the ratio values of respectively 4 and 6. Those alpha values are calculated using the method of Lecours et al. [21] (see Equations A.13 and A.14). The value b_v is the current damping value, represented either by b_{acc} or b_{dec}.

$$\alpha_a \approx \frac{c_f - c_{min}}{|\ddot{x}_d|_{max}} \tag{A.13}$$

$$\alpha_d \approx \frac{c_{max} - c_f}{|\ddot{x}_d|_{max}} \tag{A.14}$$

With c_{max} the maximum allowed damping, c_{min}, the minimum allowed damping and $|\ddot{x}_d|_{max}$ the maximum acceleration. With respectively values of: 1.0 $\frac{kgs}{rad}$, 0.5 $\frac{kgs}{rad}$ and 0.05 rad/s^2.

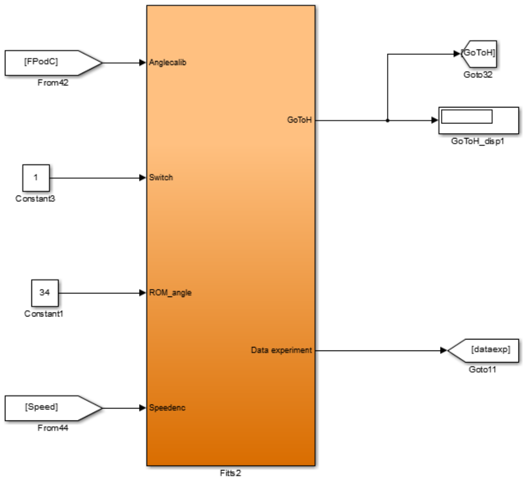

Figure A.12: Zoomed in part of the Fitts' law block in the Simulink model

A.7 Fitts' law

This block is created by S. Verros [5] and adjusted to this experiment. This block determines if the user reached the targets and home positions and sends commands to the python script. The inputs are the position based on the potentiometer, a switch constant, the maximum range of motion and the speed of the encoder. All the data regarding which target is presented, and in which state the user is, is saved in the xPC.

A.8 PID

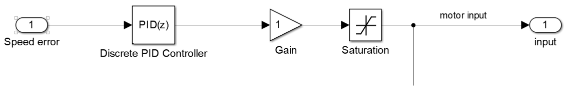

Figure A.13: Flowchart of the motor input

In Figure A.13, the flowchart of the error input to the motor input is depicted. The input is the error between the target position and the current position, determined by the motor encoder. This error is going in a PD controller and the output is used as input for the motor. The PD controller is manually tuned and P and D have respectively values of 1000 and 40. The output of the PD controller is limited with a saturation block with value 10, because the output cannot go higher than 10 V.

A.9 Output Simulink

There is one output from the model to the NI-board, this is the motor output in Volt. The NI-board sends this voltage to the Escon module 24/2 which is a servo controller.

Other outputs are variables which are saved in the xPC, these variables are e.g. speed of the encoder, potentiometer position, state of experiment etc. This data is saved on a PC after the experiment and used for data analysis. The variable names and explanations are displayed in Table A.1.

Table A.1: Saved variables Simulink

Variable name	Explanation
force	Measured force
encoder	Position measured by the encoder
podc	Position measured by the potentiometer
errorPE	Difference between potentiometer and encoder position
FN	Normalised force
MVCForce_ext	Maximum force measured during MF phase in extension direction
MVCForce_flex	Maximum force measured during MF phase in flexion direction
speed_encoder	Speed of the encoder
inputPID	Input of the PID
motor_input	Output to the motor
accadm	Acceleration determined by the admittance control law
speedadm	Speed determined by the admittance control law
angleadm	Angle determined by the admittance control law
ENC_NF	Encoder position after lowpass filter
rampneg	Negative target ramp
ramppos	Positve target ramp
filt_podc	Filtered potentiometer signal
coef1_1	Unused
coef2_1	Unused
coef1_2	First coefficient of the polyfit
coef2_2	Second coefficient of the polyfit
coef3_2	Third coefficient of the polyfit
coef4_2	Fourth coefficient of the polyfit
F_com	Force after the force compensation
F_grav	Force which is subtracted by force compensation
min_angle	Angle where force was minimum during force compensation
target_x	Pixel position of target in x-direction
target_y	Pixel position of target in y-direction
target_w	Pixel width of target
cursor_x	Pixel position of cursor in x-direction
cursor_y	Pixel position of cursor in y-direction
ID	ID of the target
trial	Trial number
seq	Trial inside block
block	Tells us in which block the experiment is
istarget	Tells us whether the target is presented or not
end_ex	Tells us when the experiment is ended
time	Gives the time of experiment
record	Tells us when the experiment starts
color	Tells us what the colors of the targets are
fitts_state	Tells us in which state the experiment is
inputforce	Inputforce to the admittance control
emg1	Gives the raw emg signal of the first electrode
emg2	Gives the raw emg signal of the second electrode
emg9	Gives the raw emg signal of the ninth electrode
emg10	Gives the raw emg signal of the tenth electrode
emg11	Gives the raw emg signal of the eleventh electrode
emg12	Gives the raw emg signal of the twelfth electrode
acc_enc	Acceleration of the encoder
offsetdegree	Value which is subtracted of the encoder during calibration
speedpodc	Speed of the potentiometer
state	Outputs the state of the Simulink model

Appendix B

Calculations of the maximum speed of the motor and the head

To see if the discrete position tracking task could be carried out with this device, the maximum speed for the motor was calculated:

$$\text{no load speed/gear ratio} = \text{rounds per minute} \tag{B.1}$$

$$12400/243 \approx 51 \text{ rpm} \tag{B.2}$$

The answer to equation B.2 will be converted to radians per second in equation B.3

$$\frac{51 * 2 * \pi}{60} = 5.34\ rad/s \tag{B.3}$$

To check the feasibility of the experiment, the maximum speed of the head in the sagittal plane has been researched. If there are no restrictions concerning the angle or the task, the head speed can go up to 10 rad/s. [22] However, the task in this paper will be conducted in a shorter range (-15 to 45 degrees) and the subjects will be asked to hold their head still when they reached the target. Therefore, literature on the head speed during a Fitts' like task has been looked into and the speeds vary from 0.21 to 1.61 rad/s [23–25], depending on the angle or direction of the head movement. As all speeds are below the calculated motor speed, it was assumed a Fitts' like experiment could be conducted with the current head support.

Appendix C

Extra figures

In this Appendix extra figures are displayed to motivate some decisions made in the paper or support results and conclusions.

C.1 Individual results muscle activity

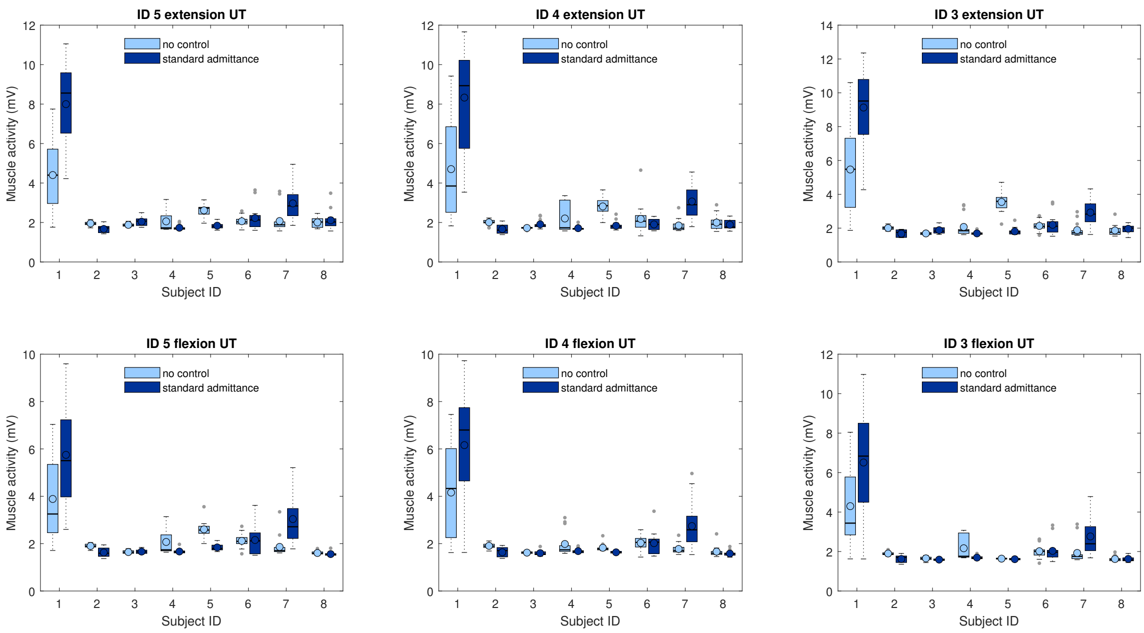

Figure C.1: Individual results for the muscle activity for the UT per direction, per target ID, per control law for all subjects. Every box plot represents 15 average values of the muscle activity (mean left and right electrode) during a trial.

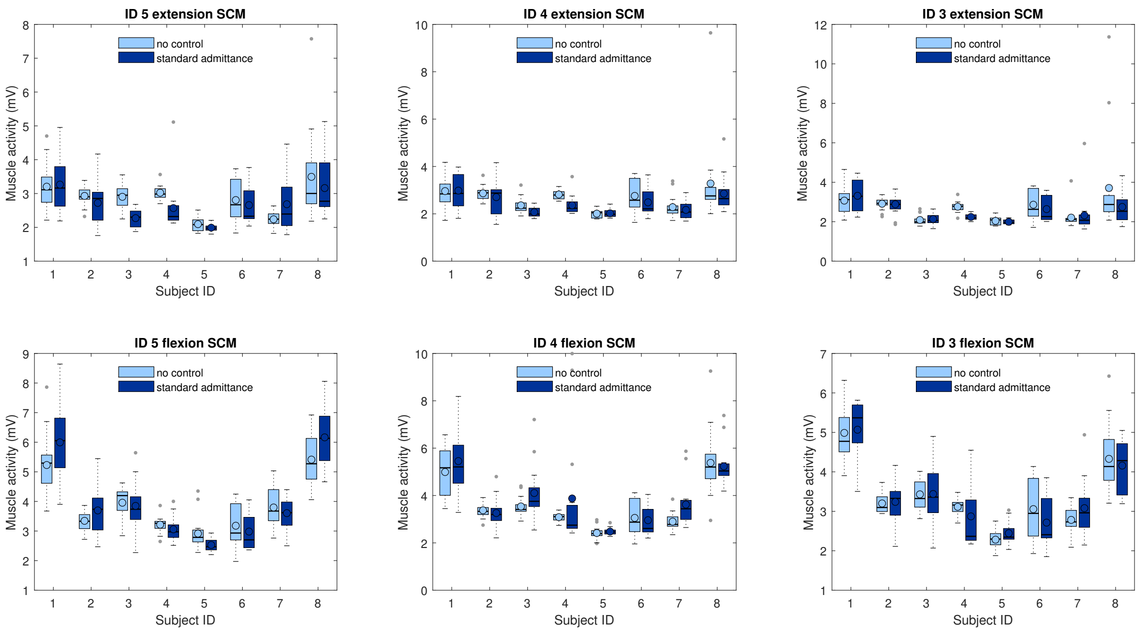

Figure C.2: Individual results for the muscle activity for the SCM per direction, per target ID, per control law for all subjects. Every box plot represents 15 average values of the muscle activity (mean left and right electrode) during a trial.

C.2 Individual results subject 6

C.2.1 EMG

Subject 6 and 8 performed the case study (3 control laws). In Figure C.3 the results of the muscle activity from subject 6 can be seen. The results of subject 8 are presented in the paper.

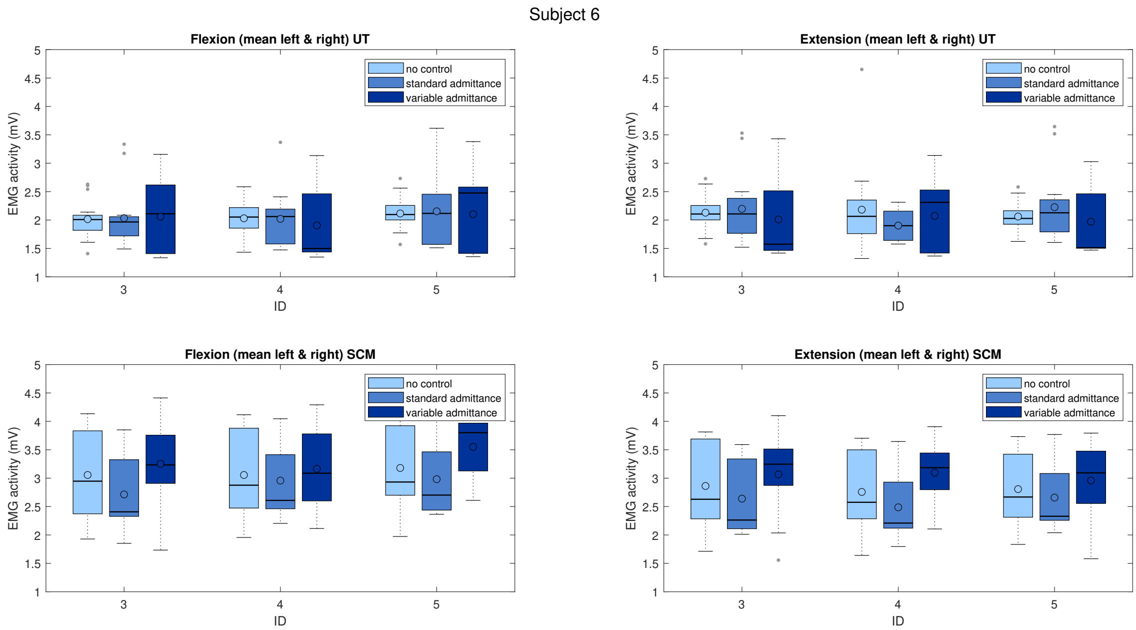

Figure C.3: Muscle activity (mV) for one subject (subject 6), per muscle, per direction, per target ID, per control law. The box plots (+ outliers) represent each 15 trials. The data points were averaged electrode voltages between the left and right side of the subject.

C.2.2 Movement Time

In Figure C.4, the results for the movement time for subject 6 are depicted. The results of subject 8 are presented in the paper.

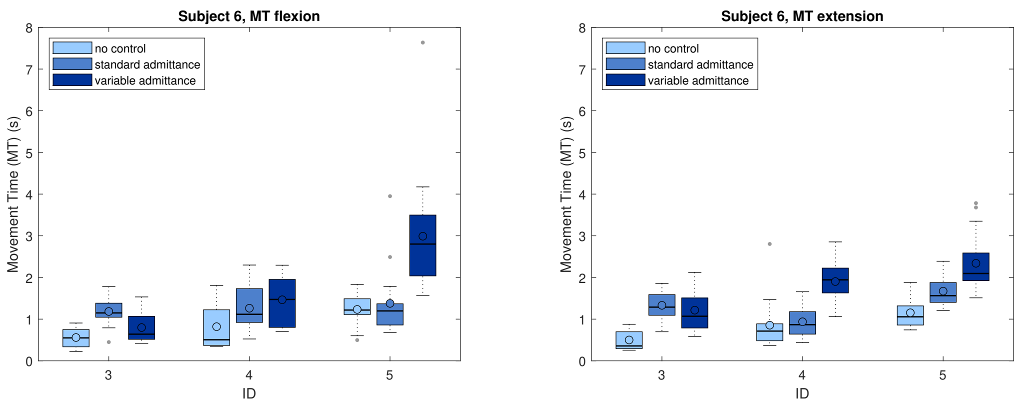

Figure C.4: Movement time (MT) for one subject (subject 6) per direction for all target ID's and control laws. Every box plot represents 15 MTs, which were the MTs per trial.

C.3 Submaximal isometric contraction (SMIC) in flexion, extension direction

Submaximal isometric contraction (SMIC) was not used in the paper, because it did not increase the validity [26] of the results. For completeness, in this paragraph more information on the SMIC of the EMG activity is presented.

In the experiment, a SMIC was performed before each trial start, during the maximum force measurements. The subjects performed the SMIC two (or three, in case of VADM) times. To see how consequent the subject pushed, the absolute difference between the measured forces, during that phase, is depicted in Figure C.5. It can be seen that some subjects showed big differences in force for the two SMICs. The repeatability of the SMIC was probably not very high due to other configurations of the head position or less muscle contraction.

Assuming that the subjects did perform at least one successful SMIC, we looked at the maximum SMIC of the two trials in the flexion and extension direction. The EMG activity was divided by the SMIC per subject and then averaged over the left and right electrode per muscle. The results are depicted in C.6. Here it can be seen that, for example, for the UT, some subjects showed an EMG percentage above 100%. This implicates that the subject did not perform a full SMIC during the MVC phase.

This and the fact that the validity of the results is not increased led to the decision that the SMIC was not used in the paper and unnormalised results were presented.

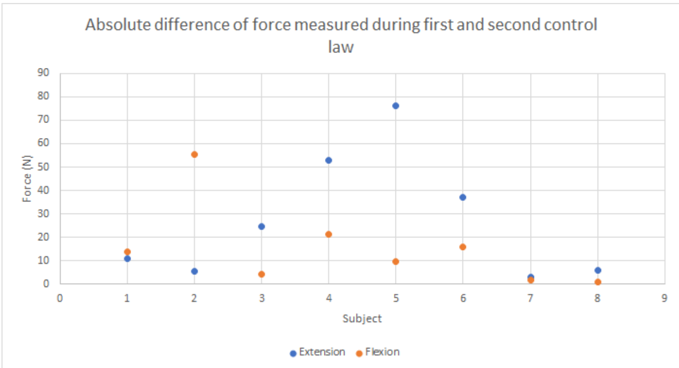

Figure C.5: Absolute difference between measured force during MVC phase in the experiment for the two control laws.

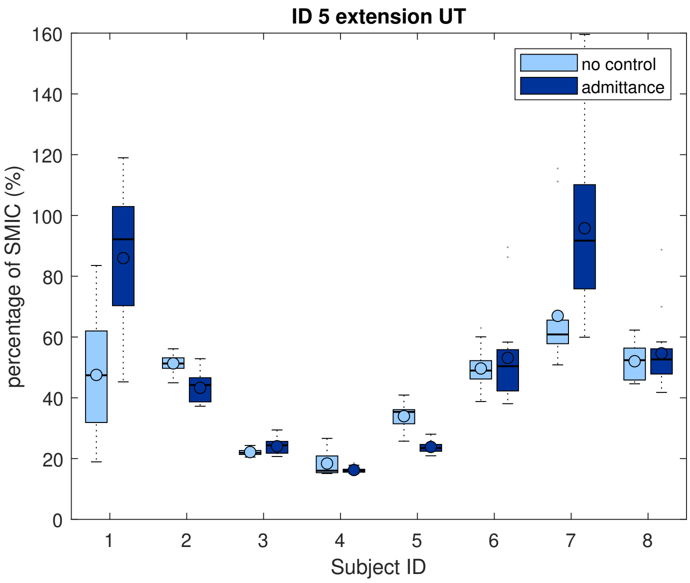

Figure C.6: Individual results for target ID 5.5 in the extension direction. The EMG activity was normalised to the maximum SMIC of the two control laws.

C.4 Individual figures overshoot case study

Subject 6 and 8 performed an extended experiment with a third control law (case study). In figure C.7 the overshoot counts per individual are presented. There is no relation seen between the amounts of overshoot and the control laws.

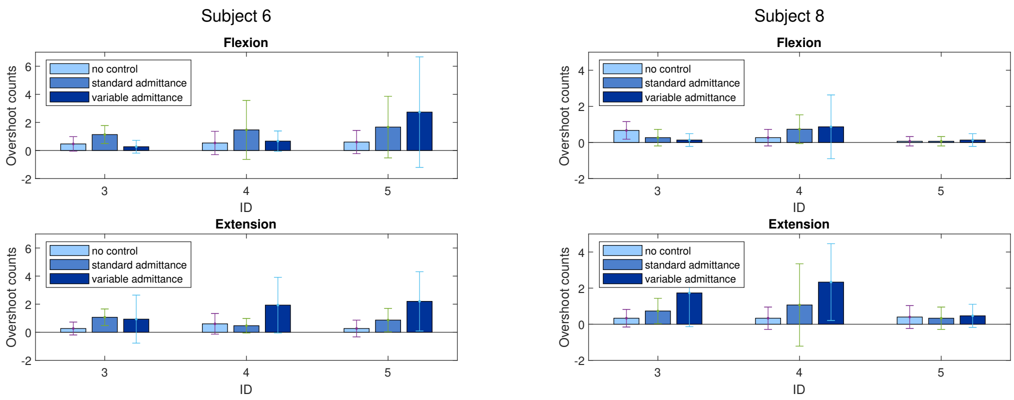

Figure C.7: Amount of overshoots per target and direction for subject 6 and 8. Every bar represent the mean for 15 trials. The error bars represent the standard deviation.

C.5 Clarification overshoot

In the paper, a graph of the amount of times subjects overshot before they reached the target, was displayed. It seemed that for SADM the overshoot rate was higher. In the discussion it was mentioned that this could be due to the noise in the potentiometer. For some subjects these overshoot numbers were very high and in Figure C.8 the movement for a subject is depicted for one target (count 30). It can be seen that the overshoot occurred because the potentiometer had a very noisy signal and as a result of that, the cursor was going in and out of the target range constantly. This has caused bias in the overshoot counts. Which probably also caused increased movement time.

In Figure C.9 the amount of overshoot is visible for every trial and all subjects per ID-direction (n = 15x8 = 120). A bigger dot represents more trials with that amount of overshoot counts. It can be seen that for ID 4 and 5 in flexion and ID 3 and 4 in extension direction several counts had high numbers. This can relate to the fact that the motor had a higher input voltage at these angles.

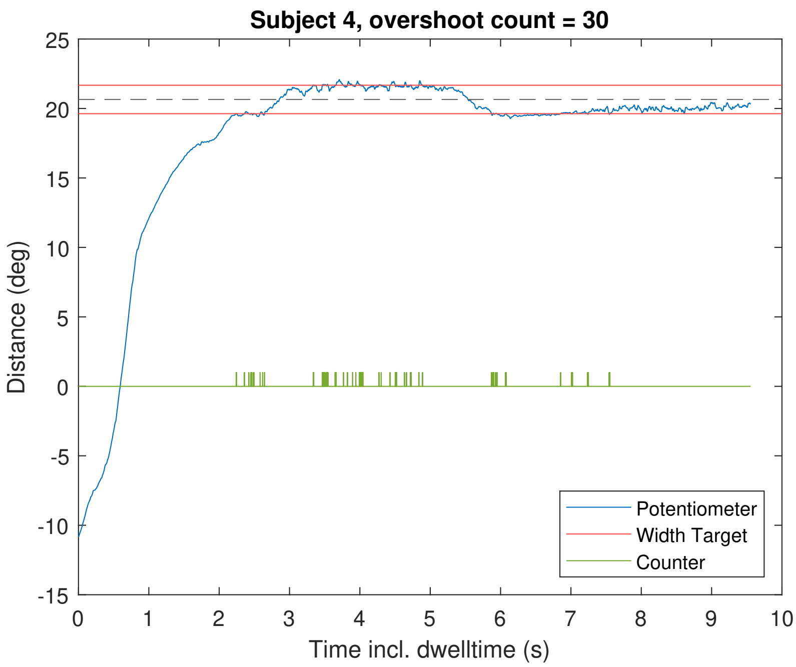

Figure C.8: Movement for one subject tracked by the filtered potentiometer. The target is represented by the horizontal lines. It could be seen that there is a lot of noise in the signal and a lot of overshoots are counted, while in reality the subject was not really overshooting every time, but really close to the border.

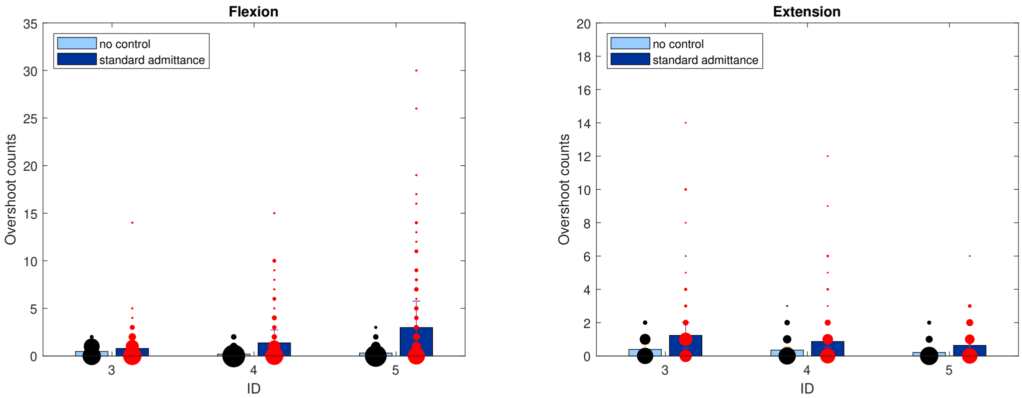

Figure C.9: Bar graph of overshoot with filled dots representing the individual counts for all trials and subjects (n = 15x8). A bigger dot represents that that amount is present more often.

C.6 Movement time over time

In Figure C.10 the average movement time over time for all subjects is depicted. Per trial, ID, direction and control law the average of all subjects is displayed with an error bar representing the standard deviation. It does not seem that movement time decreases over time. Indicating that the the familiarization block of 3 trials per ID, direction and control law is enough.

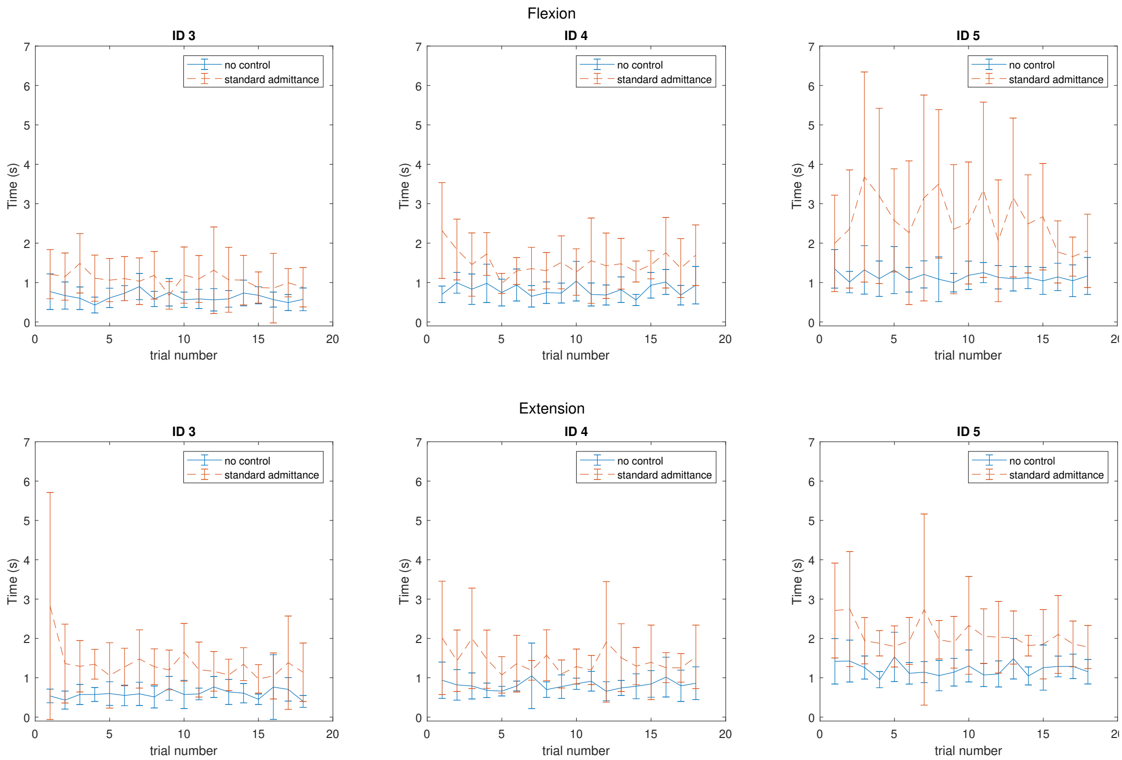

Figure C.10: Average movement time (MT) for all subjects (n=8) per direction, ID and trial. For both no control and standard admittance

C.7 Shorter dwell time

As suggested earlier, the increased movement time for SADM compared to NC could be due to the noisy potentiometer. Besides, the amount of overshoot was biased because of this noise. In this section it is investigated whether using a shorter dwell time in an offline comparison would lead to lower movement times and less overshoot.

The MT for dwell time values of 2, 1 and 0.5 seconds has been looked at (Figure C.11). It can be seen that the average movement time decreases slightly when the dwell time is decreased, however, still a significant difference between SADM and NC can be seen. The variability of the average movement times for SADM is also decreased. In Figure C.12 the overshoot for the different dwell times is depicted and it can be seen that the amount overshoot decreases for a decreased dwell time. This would indicate that the movement time is less biased by the overshoot.

This is also clearly visible in Figure C.13. The movement time is decreased a lot, because before the dwell time of 2 seconds is reached, the subject is already in the target multiple times, and for the dwell time of 0.5 seconds, this is removed. However, it can be seen that there is still some bias because the subjects had still some overshoot counts due to the noise in the potentiometer, and therefore the movement time appears still a little bit bigger. Besides, not for all cases the decreased dwell time removed the big overshoot, for example the trial in Figure C.14. Here the amount of overshoot is the same for every dwell time. Therefore the noise in the potentiometer still biased the amount of overshoots and the movement time.

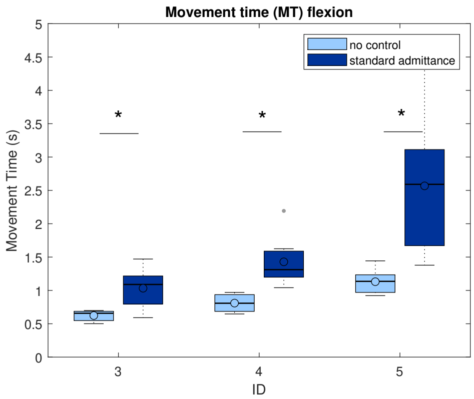

(a) Dwell time 2 seconds

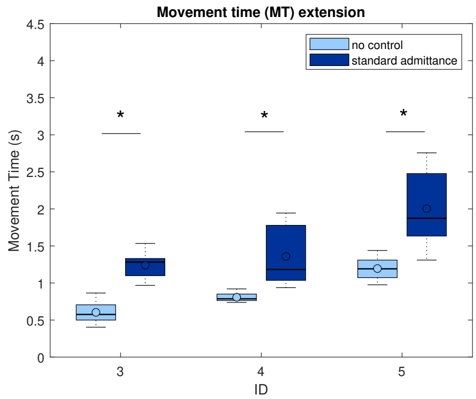

(b) Dwell time 2 seconds

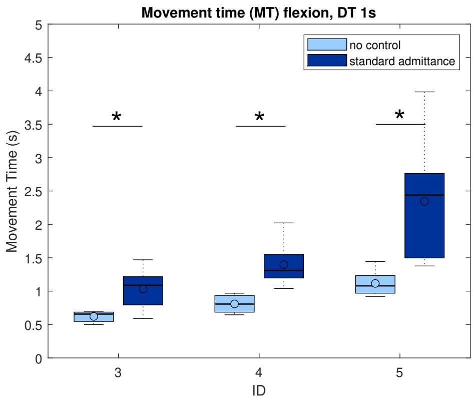

(c) Dwell time 1 second

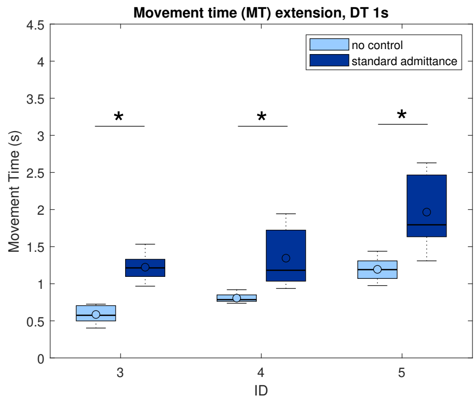

(d) Dwell time 1 second

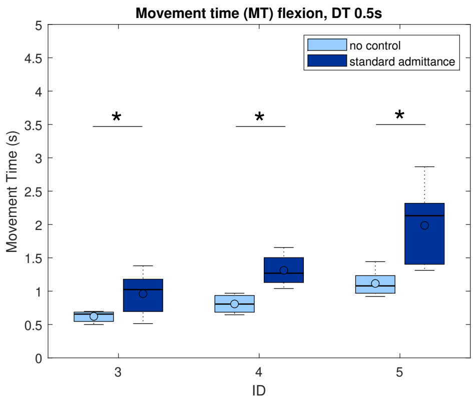

(e) Dwell time 0.5 seconds

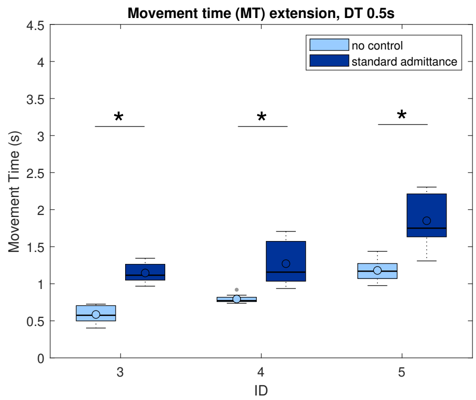

(f) Dwell time 0.5 seconds

Figure C.11: Average Movement Time (MT) for all subjects (n=8) per direction, ID and control law. Every box plot represents eight averages corresponding to all subjects. The asterisk marks a p-value < 0.05 according to the Paired T-Test. In the upper, middle and lower two figures, the movement time is depicted for a dwell time of respectively 2, 1 and 0.5 seconds.

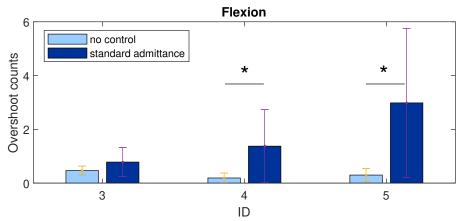

(a) Dwell time 2 seconds

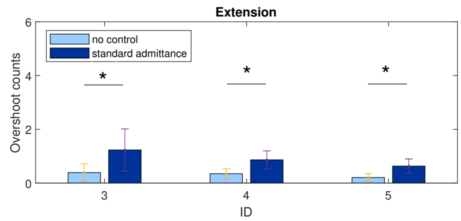

(b) Dwell time 2 seconds

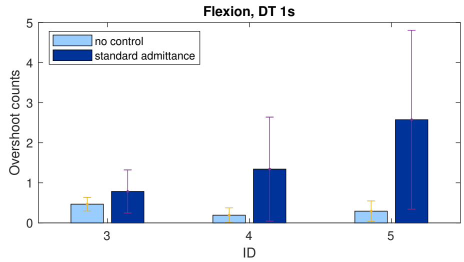

(c) Dwell time 1 second

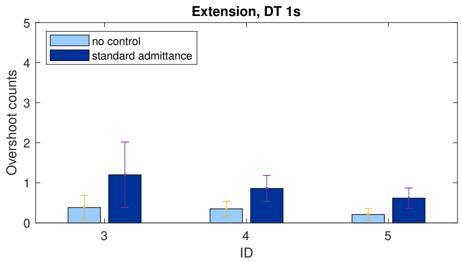

(d) Dwell time 1 seconds

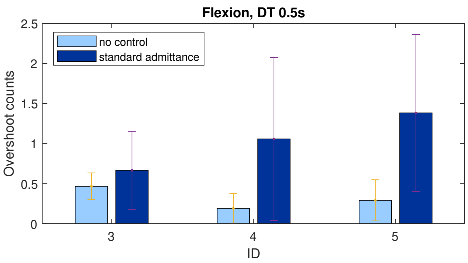

(e) Dwell time 0.5 seconds

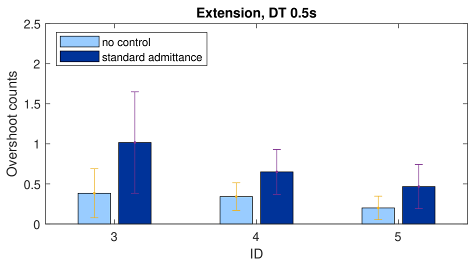

(f) Dwell time 0.5 seconds

Figure C.12: Amount of overshoots per target and direction. The mean over all subjects (n=8) was taken for this bar graph. The error bars represent the standard deviation. In the top, middle and bottom figures the overshoot for respectively dwell time of 2, 1 and 0.5 seconds is depicted.

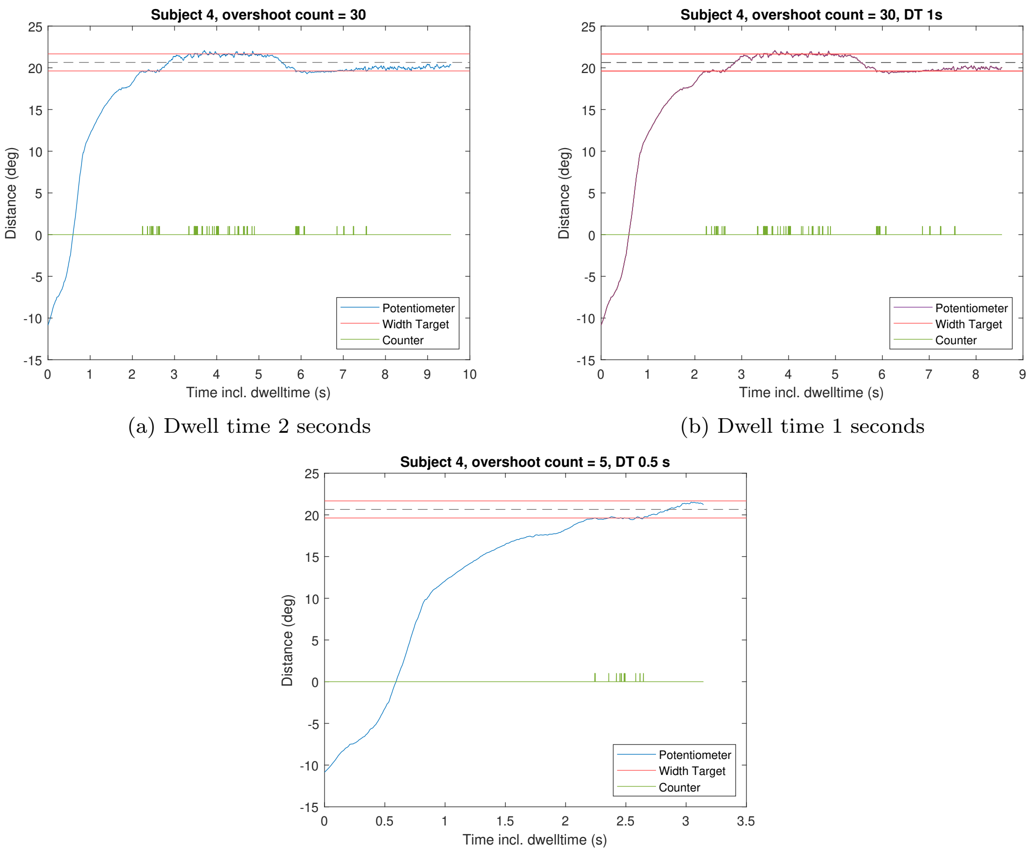

(a) Dwell time 2 seconds

(b) Dwell time 1 seconds

(c) Dwell time 0.5 seconds

Figure C.13: Movement for subject 4, trial 7 ID 5 flexion, tracked by the filtered potentiometer. The target is represented by the horizontal lines. The movement time is decreased and less overshoot is seen for a decreased dwell time. However, still too much overshoot is counted.

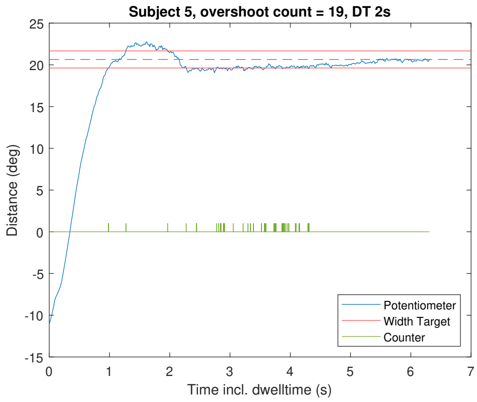

(a) Dwell time 2 seconds

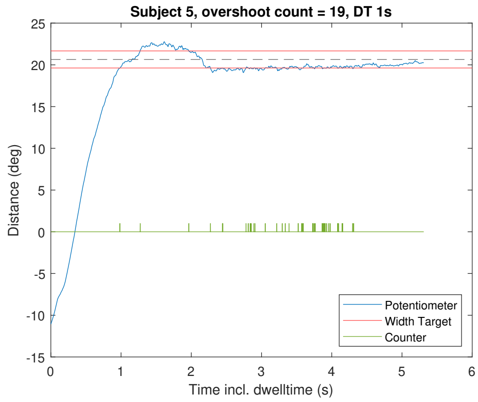

(b) Dwell time 1 second

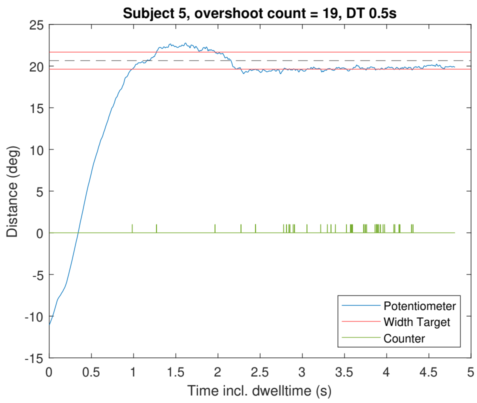

(c) Dwell time 0.5 seconds

Figure C.14: Movement for subject 5, trial 4 ID 5 flexion, tracked by the filtered potentiometer. The target is represented by the horizontal lines. A decreased dwell time did not decrease overshoot count and movement time for this subject and this trial.

C.8 Slope comparison movement

Speed of movements can have influence on the amplitude of EMG [27], therefore the slope of the movement between NC and SADM has been compared. In Figure C.15 the results for the longest target for 2 subjects in the extension direction are depicted. These results were comparable to the other results. It can be seen that for subject 3 (Figure C.15a) the slope for NC is steeper for almost all trials than that for SADM, however, for subject 6 (Figure C.15b) this cannot be said. But, one should take into account that the speed of the movement could have influenced the amplitude of the EMG, therefore biasing the results.

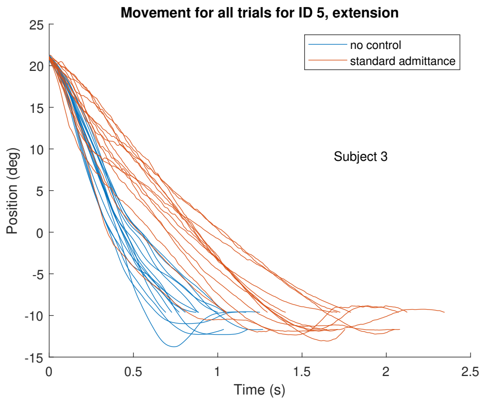

(a) Subject 3

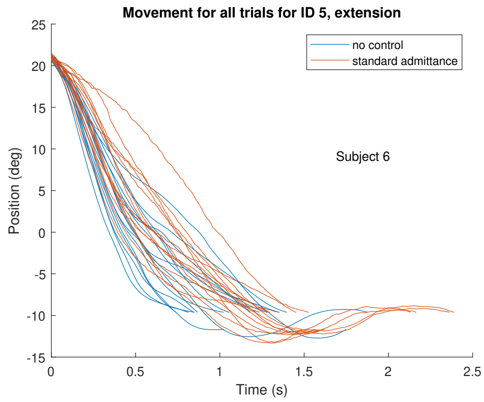

(b) Subject 6

Figure C.15: Movement for subject 3 and 6 for all trials, for ID 5, extension. For subject 3, the slope for NC is clearly steeper than that for SADM, but for subject 6 almost no differences can be seen in slope comparison.

Appendix D

Information letter

Comparing admittance control laws for an active head support with healthy subjects

Dear Sir/Madam,

With this letter, we would like to inform you about a research experiment in which the functionality of a newly developed head support device will be evaluated. This active head support is developed in order to help people suffering from neuromuscular diseases (such as Duchenne muscular dystrophy). The actuated system aims to actively support these users during movement and stabilization of the head during the activities of daily living. As these patients have weak muscles, they are unable to orient their head in the desired orientation during different activities. With the current experiment, we plan to evaluate a control algorithm for the active head support with healthy human participants. The influence of the control algorithm on muscle activity level of the neck and how fast and accurate the user can move the head while using the device will be studied. This will help us in the further development of the device.

Who we are:
This research is being carried out by the University of Twente, Biomechanical Engineering group. The experiment will take place at the Biomechatronics lab (Z127) (de Horst).

What is asked from you:
We invite you to participate in our experiment on the evaluation of an active head support. The session will require one time participation for approximately two hours. We would measure the performance of the participant using the head support in different configurations. During the session, the activity level of the neck muscles will be measured by using electromyography (EMG) and the orientation of the head support will be measured by the system. There are two phases of the experiment, in the first phase we will calibrate the system and sensors. This includes a measurement of the maximum activity level of the neck muscles and a gravity compensation measurement. In the second phase several configurations of the head support (in terms of control) will be evaluated with the use of tracking tasks (moving a cursor on a screen with head movement to go to predefined target points), to measure how fast and accurate the movements can be done while using the support system.

You will be seated in a wheelchair, and the system will be matched to your height (and head weight). To ensure a good connection between head and head support, you will wear a head band. EMG will be placed on several neck muscles to measure muscle activity. For this you are asked to bring a undershirt (shirt without sleeves). As a result of the EMG and head support it could be that some redness appears on the skin, but this will disappear after some time. Also dots for the marks of the EMG can be visible on the skin, but this can removed easily with some soap and water.

Inclusion criteria:

- Healthy adult above the age of 18
- No known history of head/neck problems
- Good visual sight (enough to see the task screen at approximately 0.5 m)

What are we going to do with the information:

The information obtained through the experiment will be used only for research purposes. The personal information of the participants will be protected and in no case, will be made public. Research data will be anonymized and only the principal investigators will have access to your personal data. Data will be stored for a period of 10 years at the University of Twente.

You can decide to stop at any point in the course of the experiment without this having any consequences for yourself and without giving any reasons. In addition, you can still decide at the end of the research and up to 24 hours thereafter, that your data may not be included in the research after all. Other relevant aspects are that your data will be handled in a confidential manner, the anonymity of your data is guaranteed and will never be disclosed to third parties without your permission.

We would greatly appreciate your participation. If you still have further questions please feel free to contact Ingrid van den Heuvel (MSc student) or Anoek Geers (daily supervisor) via email: i.s.vandenheuvel@student.utwente.nl / a.m.geers@utwente.nl or via telephone: +31 657868166.

With kind regards,
Ingrid van den Heuvel and Anoek Geers

Appendix E

Informed consent

Title research: Comparing admittance control laws for an active head support with healthy subjects

Responsible researcher	name:	Anoek Geers
	email:	a.m.geers@utwente.nl
	phone nr.:	+31 641031911
Executing researcher	name:	Ingrid van den Heuvel
	email:	i.s.vandenheuvel@student.utwente.nl
	phone nr.:	+31 657868166

To be read and signed by the subject

- I have been informed (oral or written) about the purpose, method, goal, risks and burden of the research. I also was able to ask questions and my question have been sufficiently answered. I had enough time to decide if I want to participate.

- I am aware that participation is voluntarily and that I can decide at any moment to withdraw from or quit the research. I do not need to give a reason for this.

- I am aware that some people can see my data, these people are mentioned in the information letter.

- I give consent to collection and use of my data according the goals mentioned in the information letter. I know that the data will be handled confidential and that results will only be depicted to others anonymously.

- I understand that data, results, video or photos can be used anonymously for educational purposes.

- I give consent to storage of my data for a period of 10 years after this research.

- I want to participate in this research.

Name subject:

Signature: Date : __ / __ / __

To be signed by the researcher

- I declare that I informed the subject fully about the mentioned research.
- If, during the research, data will be discovered which can influence the consent of the subject, I will inform the subject on time.

Name researcher:

Signature: Date: __ / __ / __

The subject will receive the information letter and a copy of this informed consent.

Appendix F

Questionnaire subjects

Subject info:

Name:

Age:

Length:

Gender:

Date:

Questionnaire:

Which control law was easier(1st or 2nd)?

Which control law was more tiring (1st or 2nd)?

Why was it more tiring?

I had the idea that the control law was helping/neutral/resisting:
1st:
2nd:

Appendix G

Experimental protocol

In this experimental protocol the experiment with the research question: *Comparing admittance control laws for an active head support with healthy subjects*

Preparation:

Couple of days before experiment		
1	Send participant information letter (couple of days beforehand)	
2	Reserve EMG (Delsys Trigno Wireless) (couple of days beforehand)	
Right before experiment		
3	Pick up the EMG (Delsys Trigno Wireless) from the Lopes lab	
4	Mount head support on the wheelchair	
5	Place computer screen in front of the wheelchair	
6	Plug computer screen in the power supply and the laptop and turn on screen	
7	Turn on box (electronics)	
8	Startup Matlab and Simulink script (‘Activehead’)	
9	Startup Pyzo (do not run)	
10	Plug ethernet cable into the laptop	
11	Connect EMG box to power plug	
12	Connect EMG to xPC (third NI input)	
13	Connect EMG with USB cable to laptop	
14	Turn on xPC & screen xPC	
15	Startup Trigno Control Utility	
16	Place stickers on EMG electrodes (1, 2, 9, 10)	
17	Place ‘Experiment in progress’ sign on the door	

Informing subject:

18	Welcome participant (ask if they need anything to drink)	
19	Ask if they need a bathroom break	
20	Ask if they read the information letter	
21	Ask if they have any questions	
22	Let the subjects sign the informed consent (they can read it first)	
23	Fill out participation information	
Start instructions		
24	Explain the following: • They will be seated in the robot • Head will be attached to the device • Your main job will be to do a Fitt’s like experiment (go as fast and accurate as you can to the target (and remain there) Safety instruction	

	• If something goes wrong you can press this red button and the motor will stop. There are safety measures in the script, but this is for extra safety. • You can always stop if you want to and then I can terminate the experiment. You don't have to have a reason to do this. Explain task: • I will tell you when you enter a state where you need to do something. This first state is the maximum force state. Here you will be asked to push hard against the back of the device and after to the front. Do this only with your neck and not with your back muscles. • When you're ready, it will go to the next state: a gravity compensation trajectory will be followed, where your head is going to be tilted backwards and then forwards in a very slow movement. You should relax as much as possible and let the motor do all the work. • After this, the experiment will start. You are asked to go to the target as fast as possible by moving your head up and down. The goal is reached if you stay in the target for 3 seconds. So try to stay in the target. In the beginning you will go to the end position and after a few seconds (random) the target will appear and you will need to go to the next target. This will repeated multiple times (18 + 54 + 36) and in between you have a few minutes rest. • There are two controls or three. You will do both controls, but they will be random (for every person). (For some people (2) there will be an extra control (variable admittance), this will be done after the first two)	
25	Ask if the participant has any questions	

Preparation subject:

26	Tell them that you are going to measure EMG (muscle activation) for some muscles. For that you need to put on EMG	
27	The following muscles will be used: upper trapezius (UT), 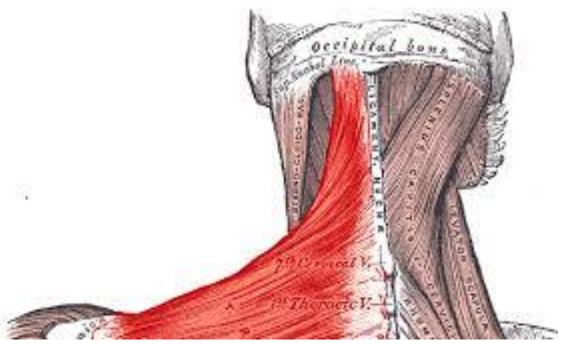 *Figure 1 https://nl.wikipedia.org/wiki/Musculus_trapezius*	

<table>
<tr><td></td><td>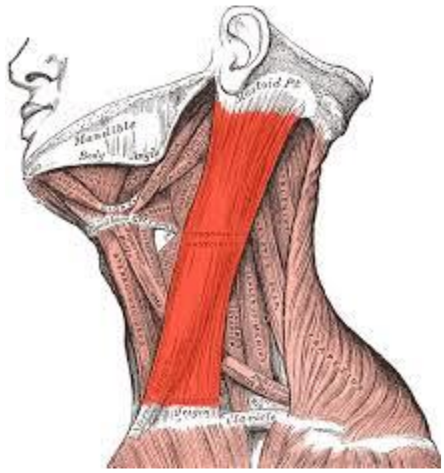
sternocleidomastoid (STR)
Figure 2 https://nl.wikipedia.org/wiki/Musculus_sternocleidomastoideus

On both sides. First the correct places needs to be determined.

For the UT: Take a measurement lineal between the C7 spline bone (the one which sticks out) and the shoulder. Place the EMG exactly in the middle. Point the arrow on the electrode towards the neck.

For the STR: The participant will be asked to look left and right. In the middle of the muscle belly (1/3rd from neck to collar bone) the EMG will be placed (and the arrow points upwards).</td><td></td></tr>
<tr><td>28</td><td>The area’s will be cleaned and/or shaved if necessary.</td><td></td></tr>
<tr><td>29</td><td>Electrode nr 1, 2, 9, 10 will be turned on before placed.</td><td></td></tr>
<tr><td>30</td><td>The electrodes will be placed on the dots in the following way:
<table><tr><th>Place</th><th>nr electrode</th></tr><tr><td>UT left</td><td>1</td></tr><tr><td>UT right</td><td>2</td></tr><tr><td>STR left</td><td>9</td></tr><tr><td>STR right</td><td>10</td></tr></table></td><td></td></tr>
<tr><td>31</td><td>Test if EMG is place correctly by starting: real_time_data_stream_plotting.m .
Let the participant put up their shoulders, look to the left and right and push against the hand forwards to see if the EMG works.</td><td></td></tr>
<tr><td>32</td><td>Participant will be seated in the wheelchair → restrict body with bands</td><td></td></tr>
<tr><td>33</td><td>Head support position will be adjusted:

In the neutral point (where the pin is in the device). The participant can look straight forward and the force sensor is horizontal. The chin of the participant should be horizontal.</td><td></td></tr>
<tr><td>34</td><td>Check if the participant is able to reach to the front and back completely, otherwise change the maximum angle during force compensation</td><td></td></tr>
</table>

35	Spring stiffness will be adjusted: The spring should feel as if going forward is just as easy as going backwards. And if head is relaxed the device can hold the head It should be on the lightest as possible: first very high, then very low. And go up until the participants tells you it feels as told.	

Experiment:

36	Look into the file 'experimental data', which control law should be first and set the correct value: 1: no control 2: admittance control 3: variable admittance control	
37	BE SURE THE STOP BUTTON IS NOT PRESSED	
38	Start Trigno control Utility	
39	Press the build model button in Simulink (see that there occur no errors)	
40	Press the connect to target button in Simulink	
41	Make sure the pin is in the device!	
42	Run the Simulink script	
43	Run the Pyzo script	
44	If state 3 is reached, tell the participant to perform the MF (hold the device a bit, so there is not too much stress on the setup)	
45	After the MVC, remove the pin!!!	
46	Before going to state 4 (press the switch), mention to the participant to relax completely	
47	The force compensation state is busy → participant should relax completely!	
48	Before going to the experiment state, set up the experiment screen: set value switch for Fitt's law at 0 and then 1.	
49	Tell the participant that first the practice block will start. Ask if the participant is ready (if yes, press switch). Participant can start the experiment. Assignment is to do the task as fast and accurate as possible!!	
50	After 1 block of 18 trials (you can see this on the screen), the familiarization blocks are over. IF IT GOES INTO THE ERROR STATE: STATE 10 Bring back the participant to the neutral position: - put in pin Push the switch button which goes to the calibration state. It then automatically goes to state 9 after which the pin can be removed. Then pressing the switch again will activate the experiment once more.	
51	Give rest to the participant for 1 minute	
52	Set the switch value for Fitt's law back to 0. Perform calibration as told above and then set the switch value to 1 again. The first 3 blocks of the real experiment will start. Tell them that!	

53	After 3 blocks give rest for 1 minute and perform calibration and then perform step 51 & 52 again for 2 more blocks	
54	Encourage once in a while	
55	After this first experiment is finished (check state Fitts = 15), click the stop button and save the data with the following filename: 'subjectnr_controllawnr_date'	
56	Close the Pyzo script by clicking with the left mouse button in the shell environment and press terminate and after close.	
57	Before you can use the Pyzo script again a new shell needs to be opened.	
58	Perform step 36 till 57 again once more for the other control law. If already repeated go to step 60. Give participants a longer break (head band can be removed to relax a bit. Break of 5 minutes)	
59	For some participants a third control law is added and for this repeat step 36 till 57 again, with the third control law. If this I not needed repeat to step 60	

Finishing up:

60	Remove the head band from the participant	
61	Remove the EMG electrodes	
62	Let the participant fill in the questionnaire	
63	Remove stickers from the electrodes and put them back in the box	
64	Turn off the xPC and the box (electronics)	
65	Bring back the EMG to the Lopes lab	

Bibliography

[1] "The headmaster collar," https://www.symmetric-designs.com/headmaster-collar, Accessed: 21-05-2019.

[2] "Necksolutions headrest," https://www.necksolutions.com/wheelchair-headrests/, Accessed: 21-05-2019.

[3] "Focal modular headrest," https://www.focalmeditech.nl/en/modular-headrests, Accessed: 21-05-2019.

[4] K. Anam and A. A. Al-Jumaily, "Active exoskeleton control systems: State of the art," *Procedia Engineering*, vol. 41, pp. 988 – 994, 2012, international Symposium on Robotics and Intelligent Sensors 2012 (IRIS 2012). [Online]. Available: http://www.sciencedirect.com/science/article/pii/S1877705812026732

[5] P. G. Van Lenthe, S. Verros, E. E. G. Hekman, R. Carloni, and H. F. J. M. Koopman, "Comparing assistive admittance control algorithms for a trunk supporting exoskeleton," in *2018 IEEE International Conference on Robotics and Automation (ICRA)*, May 2018, pp. 2828–2834.

[6] J. Lobo Prat, P. Kooren, M. Janssen, A. Keemink, P. Veltink, A. Stienen, and H. Koopman, "Implementation of emg- and force-based control interfaces in active elbow supports for men with duchenne muscular dystrophy: a feasiblitity study," *IEEE transactions on neural systems and rehabilitation engineering*, vol. 24, no. 11, pp. 1179–1190, 11 2016.

[7] J. Lobo-Prat, P. N. Kooren, A. Q. L. Keemink, M. I. Paalman, E. E. G. Hekman, P. H. Veltink, A. H. A. Stienen, and B. F. J. M. Koopman, "Design and control of an experimental active elbow support for adult duchenne muscular dystrophy patients," in *5th IEEE RAS/EMBS International Conference on Biomedical Robotics and Biomechatronics*, Aug 2014, pp. 187–192.

[8] J. Lobo-Prat, A. Keemink, A. Ha Stienen, A. Schouten, P. H Veltink, and B. Hfjm Koopman, "Evaluation of emg, force and joystick as control interfaces for active arm supports," *Journal of neuroengineering and rehabilitation*, vol. 11, p. 68, 04 2014.

[9] G. Aguirre-Ollinger, U. Nagarajan, and A. Goswami, "An admittance shaping controller for exoskeleton assistance of the lower extremities," *Autonomous Robots*, vol. 40, no. 4, pp. 701–728, Apr 2016. [Online]. Available: https://doi.org/10.1007/s10514-015-9490-8

[10] P. M. Fitts, "The information capacity of the human motor system in controlling the amplitude of movement." *Journal of Experimental Psychology: General*, vol. 121, no. 3, pp. 262 – 269, 1992.

[11] R. J. Jagacinski and J. M. Flach, *Control theory for humans.* Lawrence Erlbaum Associates, Inc.

[12] R. J. Jagacinski and D. L. Monk, "Fitts' law in two dimensions with hand and head movements movements," *Journal of Motor Behavior*, vol. 17, no. 1, pp. 77–95, 1985, pMID: 15140699. [Online]. Available: https://doi.org/10.1080/00222895.1985.10735338

[13] M. Takeda, T. Sato, H. Saito, and et al., "Explanation of fitts' law in reaching movement based on human arm dynamics," *Sci Rep*, vol. 9, 2019.

[14] R. Kerr, "Diving, adaptation, and fitts law," *Journal of Motor Behavior*, vol. 10, no. 4, pp. 255–260, 1978, pMID: 15186987. [Online]. Available: https://doi.org/10.1080/00222895.1978.10735159

[15] S. Verros, N. Mahmood, L. Peeters, J. Lobo-Prat, A. Bergsma, E. Hekman, G. J. Verkerke, and B. Koopman, "Evaluation of control interfaces for active trunk support," *IEEE Transactions on Neural Systems and Rehabilitation Engineering*, vol. 26, no. 10, pp. 1965–1974, Oct 2018.

[16] A. Q. L. Keemink, R. I. K. Fierkens, J. Lobo-Prat, J. S. F. Schorsch, D. A. Abbink, J. B. J. Smeets, and A. H. A. Stienen, "Using position dependent damping forces around reaching targets for transporting heavy objects: A fitts' law approach," in *2016 6th IEEE International Conference on Biomedical Robotics and Biomechatronics (BioRob)*, June 2016, pp. 1323–1329.

[17] R. G. Radwin, G. C. Vanderheiden, and M.-L. Lin, "A method for evaluating head-controlled computer input devices using fitts' law," *Human Factors*, vol. 32, no. 4, pp. 423–438, 1990, pMID: 2150065. [Online]. Available: https://doi.org/10.1177/001872089003200405

[18] I. S. MacKenzie, "A note on the information-theoretic basis for fitts' law," *Journal of Motor Behavior*, vol. 21, no. 3, pp. 323–330, 1989, pMID: 15136269. [Online]. Available: https://doi.org/10.1080/00222895.1989.10735486

[19] G. Aguirre-Ollinger, J. E. Colgate, M. A. Peshkin, and A. Goswami, "Inertia compensation control of a one-degree-of-freedom exoskeleton for lower-limb assistance: Initial experiments," *IEEE Transactions on Neural Systems and Rehabilitation Engineering*, vol. 20, no. 1, pp. 68–77, Jan 2012.

[20] Y. Zhuang, S. Yao, C. Ma, and R. Song, "Admittance control based on emg-driven musculoskeletal model improves the human–robot synchronization," *IEEE Transactions on Industrial Informatics*, vol. 15, no. 2, pp. 1211–1218, Feb 2019.

[21] A. Lecours, B. Mayer-St-Onge, and C. Gosselin, "Variable admittance control of a four-degree-of-freedom intelligent assist device," in *2012 IEEE International Conference on Robotics and Automation*, May 2012, pp. 3903–3908.

[22] F. Hernandez and D. B. Camarillo, "Voluntary head rotational velocity and implications for brain injury risk metrics," *Journal of Neurotrama*, vol. 36, 03 2019.

[23] R. Radwin, G. Vanderheiden, and M. L Lin, "A method for evaluating head-controlled computer input devices using fitts' law," *Human factors*, vol. 32, pp. 423–38, 09 1990.

[24] M. R. Williams and R. F. Kirsch, "Evaluation of head orientation and neck muscle emg signals as command inputs to a human–computer interface for individuals with high tetraplegia," *IEEE Transactions on Neural Systems and Rehabilitation Engineering*, vol. 16, no. 5, pp. 485–496, Oct 2008.

[25] E. R. Hoffmann, A. H. S. Chan, and P. T. Heung, "Head rotation movement times," *Human Factors*, vol. 59, no. 6, pp. 986–994, 2017, pMID: 28796975. [Online]. Available: https://doi.org/10.1177/0018720817701000

[26] M. Halaki and K. Ginn, "Normalization of emg signals: To normalize or not to normalize and what to normalize to?" in *Computational Intelligence in Electromyography Analysis*, G. R. Naik, Ed. Rijeka: IntechOpen, 2012, ch. 7. [Online]. Available: https://doi.org/10.5772/49957

[27] T. Masuda, T. Kizuka, J. Y. Zhe, H. Yamada, K. Saitou, T. Sadoyama, and M. Okada, "Influence of contraction force and speed on muscle fiber conduction velocity during dynamic voluntary exercise," *Journal of Electromyography and Kinesiology*, vol. 11, no. 2, pp. 85 – 94, 2001. [Online]. Available: http://www.sciencedirect.com/science/article/pii/S1050641100000481